

DEXH Box RNA Helicase–Mediated Mitochondrial Reactive Oxygen Species Production in *Arabidopsis* Mediates Crosstalk between Abscisic Acid and Auxin Signaling

Junna He,^a Ying Duan,^a Deping Hua,^a Guangjiang Fan,^a Li Wang,^a Yue Liu,^a Zhizhong Chen,^a Lihua Han,^{b,c} Li-Jia Qu,^{b,c} and Zhizhong Gong^{a,c,d,1}

^aState Key Laboratory of Plant Physiology and Biochemistry, College of Biological Sciences, China Agricultural University, Beijing 100193, China

^bState Key Laboratory of Protein and Plant Gene Research, College of Life Sciences, Peking University, Beijing 100871, China

^cNational Center for Plant Gene Research, Beijing 100193, China

^dChina Agricultural University–Purdue University Joint Research Center, Beijing 100193, China

It is well known that abscisic acid (ABA) promotes reactive oxygen species (ROS) production through plasma membrane-associated NADPH oxidases during ABA signaling. However, whether ROS from organelles can act as second messengers in ABA signaling is largely unknown. Here, we identified an ABA overly sensitive mutant, *abo6*, in a genetic screen for ABA-mediated inhibition of primary root growth. *ABO6* encodes a DEXH box RNA helicase that is involved in regulating the splicing of several genes of complex I in mitochondria. The *abo6* mutant accumulated more ROS in mitochondria, as established using a mitochondrial superoxide indicator, circularly permuted yellow fluorescent protein. Two dominant-negative mutations in *ABA insensitive1 (abi1-1)* and *abi2-1* greatly reduced ROS production in mitochondria. The ABA sensitivity of *abo6* can also be compromised by the *atrbohF* mutation. ABA-mediated inhibition of seed germination and primary root growth in *abo6* was released by the addition of reduced GSH and exogenous auxin to the medium. Expression of auxin-responsive markers *ProDR5:GUS* (for synthetic auxin response element D1–4 with site-directed mutants in the 5'-end from soybean): β -glucuronidase) and *Indole-3-acetic acid inducible2:GUS* was greatly reduced by the *abo6* mutation. Hence, our results provide molecular evidence for the interplay between ABA and auxin through the production of ROS from mitochondria. This interplay regulates primary root growth and seed germination in *Arabidopsis thaliana*.

INTRODUCTION

One of the most important traits of a crop plant is the root system. The root system determines the efficiency of nutrient and water uptake from soil and influences the distribution of photosynthates throughout the plant. Root growth is regulated by hormones and environmental conditions (Teale et al., 2008; Fukaki and Tasaka, 2009). The phytohormone abscisic acid (ABA) plays crucial roles in regulating root growth and also helps regulate seed dormancy and germination, stomatal movement, vegetative growth, and responses to biotic and abiotic stress (Zhu, 2002; Ton et al., 2009; Cutler et al., 2010; Kim et al., 2010). Although ABA is required for root growth and ABA-deficient mutants have reduced root systems (Xiong and Zhu, 2003), high concentrations of exogenous ABA inhibit root growth. Our understanding of how ABA stimulates or inhibits seed germination,

seedling growth, and stomatal movement has been greatly enhanced by genetic and molecular analyses; however, our understanding remains incomplete (Zhu, 2002; Chinnusamy et al., 2008; Cutler et al., 2010; Kim et al., 2010).

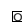
ABA stimulates the production of reactive oxygen species (ROS; including O_2^- and hydrogen peroxide [H_2O_2]) through plasma membrane-localized NADPH oxidases (Kwak et al., 2003). These ROS act as important second messengers in regulating root growth, stomatal movement, and seed germination in the ABA signaling pathway (Kwak et al., 2003). Mutations in two NADPH oxidases, respiratory burst oxidase homologs D and F (RBOHD/F), reduce ROS production, and *Arabidopsis thaliana rbohF* single or *rbohD rbohF* double mutants are insensitive to ABA-mediated inhibition of root growth (Kwak et al., 2003). The ABA-activated SnRK2 protein kinase OPEN STOMATA1 (OST1) interacts with and phosphorylates RBOHF, suggesting that RBOHF is regulated by OST1 (Sirichandra et al., 2009). The activities of ABA INSENSITIVE1 (ABI1) and ABI2, two critical negative regulators in the ABA signaling pathway, are inhibited by the H_2O_2 in vitro (Meinhard and Grill, 2001; Meinhard et al., 2002). ABI2 interacts with GPX3 (the glutathione peroxidase 3 that regulates the redox state of guard cells) (Miao et al., 2006), and ABI1 binds to phosphatidic acid produced by phospholipase $D\alpha 1$ (Zhang et al., 2004; Zhang et al., 2009). Phosphatidic acid interacts with and stimulates RBOHD/F for ROS production (Zhang et al., 2009). A mutation in RBOHC results in

¹ Address correspondence to gongzz@cau.edu.cn.

The author responsible for distribution of materials integral to the findings presented in this article in accordance with the policy described in the Instructions for Authors (www.plantcell.org) is: Zhizhong Gong (gongzz@cau.edu.cn).

 Some figures in this article are displayed in color online but in black and white in the print edition.

 Online version contains Web-only data.

 Open Access articles can be viewed online without a subscription.

www.plantcell.org/cgi/doi/10.1105/tpc.112.098707

ROS reduction, inhibition of root hair growth, and reduced activities of Ca^{2+} channels in root hairs, suggesting that ROS regulate plant cell expansion by activating Ca^{2+} channels (Foreman et al., 2003). A recent study on a plasma membrane-associated Pro-rich extensin-like receptor kinase 4 also suggests that Ca^{2+} is important for root growth in the ABA signaling pathway (Bai et al., 2009). In both the *rbohC* mutant and the *rbohD rbohF* double mutant, the root lengths are greatly reduced, suggesting that ROS are required for plant root growth (Foreman et al., 2003; Kwak et al., 2003). A recent study on ROS production as mediated by the basic helix-loop-helix transcriptional factor UPBEAT1 indicates that ROS control the transition from cell proliferation to differentiation in roots via a separate pathway that involves auxin signaling (Tsukagoshi et al., 2010). ROS are also produced by fatty acid β -oxidation and glycolate oxidases in peroxisomes and by electron transport in the chloroplasts and mitochondria (Laloi et al., 2004). The biological roles of these ROS in the ABA signaling pathway are largely unknown.

In the mitochondrial electron transport chain, complex I and III are major sites for ROS production in darkness and in tissues lacking chloroplasts (Laloi et al., 2004). Impairment of the components in this chain leads to the accumulation of ROS in mitochondria. Because the mitochondrial electron transport chain also contains an alternative oxidase that can be activated under stress to remove toxic ROS (Maxwell et al., 1999), ROS produced from mitochondria are present only in low concentrations in green tissues (Apel and Hirt, 2004).

Most mitochondrial proteins are encoded by nuclear genes, and only a small number are encoded by mitochondrial genes. The mitochondrial pre-RNAs require processing to become mature RNAs. The processing of mitochondrial RNAs, including intron splicing and RNA editing, requires the help of many nuclear proteins, such as DEAD box RNA helicases (Köhler et al., 2010) and pentatricopeptide repeat (PPR) proteins (Liu et al., 2010). DEAD/DEXH box RNA helicases, which require the help of other proteins and ATP hydrolysis, act as molecular motors that rearrange inter- or intramolecular RNA secondary structures or that dissolve RNA-protein complexes. Only a few RNA helicases have been analyzed in *Arabidopsis*. LOW EXPRESSION OF OSMOTICALLY RESPONSIVE GENES4 is required for mRNA export from the nucleus to the cytoplasm (Gong et al., 2002, 2005), and STRESS-RESPONSE SUPPRESSOR1 (*STRS1*) and *STRS2* are involved in the response to many abiotic stresses (Kant et al., 2007). Another RNA helicase, PUTATIVE MITOCHONDRIAL RNA HELICASE2, is involved in group II intron splicing in mitochondria (Köhler et al., 2010). Mutation in the RNA helicase SIZE EXCLUSION LIMIT1 leads to increased ROS- and plasmodesmata-mediated cell-cell transport and embryo death (Stonebloom et al., 2009). However, the molecular roles of most of these RNA helicases are unknown.

To study the molecular mechanisms by which ABA regulates primary root growth, we performed a genetic screen in which we identified mutants that are sensitive or insensitive to ABA inhibition of primary root growth. As reported previously, we identified several ABA-overly sensitive (*abo*) mutants for ABA inhibition of primary root growth (Yin et al., 2009; Zhou et al., 2009; Liu et al., 2010; Ren et al., 2010; Wang et al., 2011). Among them, *ABO5* encodes a PPR protein required for cis-splicing of mitochondrial *nad2* intron 3 (Liu et al., 2010). In this

study, we characterized another *abo* mutant, *abo6*. *ABO6* encodes a DEXH box RNA helicase that is localized in the mitochondria and is required for splicing of several genes in complex I. *abo6* mutants accumulated more ROS than the wild type in the mitochondria, while ABA treatment enhanced ROS accumulation, and impairing ABA signaling by the *abi1-1* or *abi2-1* dominant-negative mutation reduced ROS accumulation, as indicated by a mitochondrial superoxide indicator circularly permuted yellow fluorescent protein (cpYFP) (Wang et al., 2008). The addition of reduced GSH (a reducing chemical) to the medium rescued ABA inhibition of primary root growth, while addition of the GSH inhibitor buthionine sulphoximine (BSO) enhanced the ABA inhibition of primary root growth. Further analyses suggested that ABA-mediated inhibition of primary root growth involves auxin homeostasis. Together, these results indicate that, like the ROS produced by plasma membrane NADPH oxidases, the ROS produced by mitochondria are important second messengers in the ABA signaling pathway.

RESULTS

Isolation of *abo6*

abo6 was isolated during a genetic screen for ABA-sensitive mutants; the screen used a root-bending assay on Murashige and Skoog (MS) medium containing 30 μM ABA (Yin et al., 2009). We compared the root growth of 4-d-old wild-type and *abo6* seedlings transferred onto MS medium supplemented with different concentrations of ABA for 7 d. As shown in Figures 1A and 1B, although *abo6* had shorter primary roots than the wild type on MS medium without ABA (see Supplemental Figure 1 online), primary root growth was more sensitive in *abo6* than in the wild type to ABA (Figure 1A). In addition, seed germination greening (greening cotyledon ratio) was more sensitive in *abo6* than in the wild type to ABA (Figures 1C and 1D) and to NaCl and mannitol (Figures 1E to 1G). *abo6* plants were later flowering than the wild type (see Supplemental Figure 1 online).

We analyzed whether *abo6* was more drought resistant than the wild type. *abo6* and wild-type plants were grown in pots under water sufficient conditions. After 2 weeks, the plants were subjected to drought stress by withholding water. After 10 d of drought treatment, the wild-type leaves showed clear wilting signs, but *abo6* leaves remained turgid (Figure 2A). Because the *abo6* mutants were slightly smaller than the wild-type plants, and because leaf surface area affects the rate of transpiration from leaves, we measured the water loss of detached leaves so as to obtain a direct measure of transpiration. The rate of water loss was slower from detached *abo6* leaves than from detached wild-type leaves (Figure 2B), which was consistent with the drought-tolerant phenotype of *abo6* plants growing in soil. Under water-sufficient conditions, the stomatal apertures of *abo6* were smaller than those of the wild type (Figure 2C). We also found that Pro and soluble sugar contents were greater in *abo6* than in the wild type under both water-sufficient and drought conditions (Figures 2D and 2E). These results suggest that the *abo6* mutant suffers from constitutive stress and also partially explain its drought-tolerant phenotype.

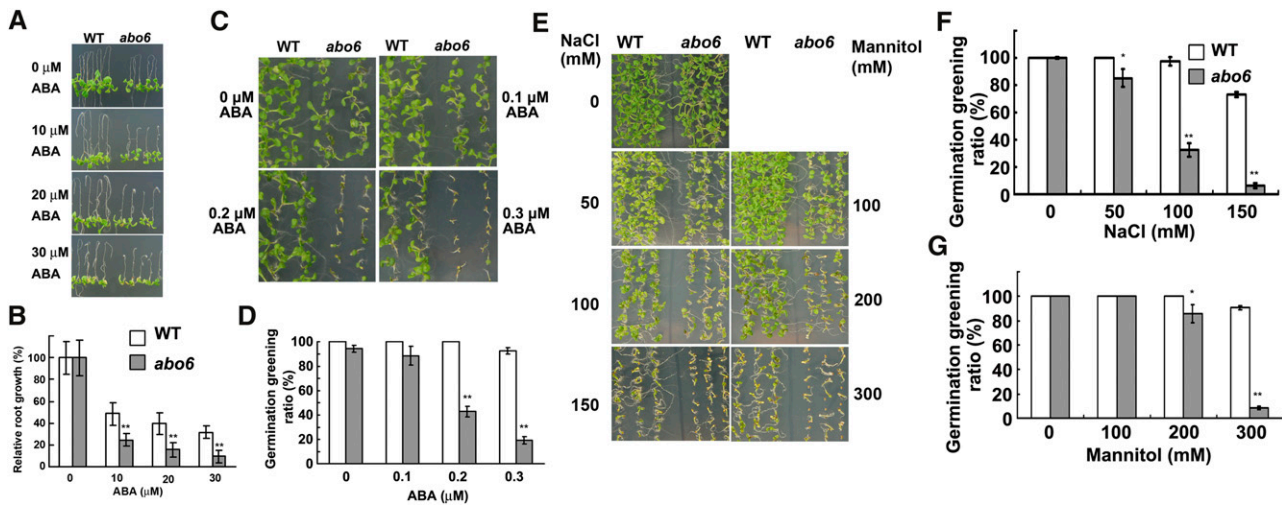


Figure 1. Primary Root Growth and Seed Germination of *abo6* and the Wild Type.

(A) Primary root growth of seedlings grown on MS medium or MS medium supplemented with 10, 20, and 30 μM ABA. Four-day-old seedlings were transferred to the different media and grown for 7 d before being photographed. WT, the wild type.

(B) Relative primary root growth of *abo6* or wild-type seedlings grown on medium containing different concentrations of ABA (plates were oriented vertically with root tips down). Values are means \pm SE (growth without ABA was set to 100%). About 10 roots were measured in each of three plates, and three independent experiments were performed. Data are means \pm SE of three biological repetitions. ** $P < 0.01$.

(C) Germination greening of *abo6* and the wild type on MS medium containing different concentrations of ABA. Plates were removed from 4°C and kept in a growth chamber for 7 d before they were photographed.

(D) Statistical analysis of the seed germination greening ratio in **(C)**.

(E) Seed germination greening as affected by different concentrations of NaCl or mannitol. The plates were kept in a growth chamber for 7 d before they were photographed.

(F) and **(G)** Statistical analysis of seed germination greening ratio in **(E)**.

For seed germination greening in **(D)**, **(F)**, and **(G)**, ~ 30 seeds were counted in each of three plates for one experiment, and three independent experiments were performed with similar results. Data are means \pm SE of three biological repetitions. * $P < 0.05$; ** $P < 0.01$.

[See online article for color version of this figure.]

ABO6 Encodes a DEXH RNA Helicase That Is Localized to Mitochondria

The *abo6* mutant (in the Columbia *gl1* accession) was crossed with the Landsberg accession. The F2 seedlings that showed ABA sensitivity in root growth (on MS medium supplemented with 30 μM ABA) were selected. *ABO6* was initially mapped to the upper arm of chromosome 5 and was precisely mapped to the BAC clones MUK11 and MUG13 (Figure 3A). We sequenced all of the open reading frames in this region and identified a G1575-to-A1575 (counting from the first putative ATG) mutation in the sixth exon of *AT5G04895*; this mutation caused a Gly334-to-Glu334 change in *AT5G04895*.

ABO6 was annotated as a DEAD box RNA helicase that contains a DEXH box (Figure 3B). There are 58 DEAD box proteins in *Arabidopsis*, most of which belong to the sf2 family, a family that is divided into DEAD, DEAH, and DEXD/H subfamilies (Boudet et al., 2001; Mingam et al., 2004). The *abo6* mutation Gly-334 to Glu-334 occurs in the DEXH region. Gly-334 is a well-conserved amino acid in the DEXH region of *ABO6* homologs from different species (Figure 3B). The cDNA of *AT5G04895* was amplified and overexpressed under the control of a super promoter in *abo6*. We obtained 22 independent transgenic lines and selected several T3 homozygous lines to

test for ABA sensitivity of root growth: All were rescued to the wild-type phenotype on MS medium containing 30 μM ABA. As an example, the homozygous transgenic line 9 complemented both the ABA-sensitive phenotype (Figures 3C and 3D) and the retarded-growth phenotype (Figure 3E), indicating that the ABA-sensitive phenotype of *abo6* was caused by the mutation in *AT5G04895*. We obtained T-DNA lines but failed to obtain homozygous T-DNA insertion plants, suggesting that *ABO6* is required for plant survival. We crossed *abo6* with a heterozygous T-DNA mutant (Figure 3A) and analyzed the F1 plants for root sensitivity to ABA. We found that the ratio of normal plants to sensitive plants was near 1:1 (36:38) (Figure 3F). The ABA-sensitive plants were heterozygous in that they carried both the *abo6* mutation and the T-DNA insertion. Together, these results confirmed that *AT5G04895* is *ABO6*.

ABO6 is predicted to localize to mitochondria, according to the program TargetP (<http://www.cbs.dtu.dk/services/TargetP>). To verify this result, we fused the N terminus (nucleotides 1 to 1227) of the *abo6* cDNA fragment (including a putative signal peptide) in frame with green fluorescent protein (GFP) under the control of a super promoter. The constructs were transiently transformed into *Arabidopsis* protoplasts stained with MitoTracker Red, a dye that specifically accumulates in mitochondria. The green fluorescence of the fusion protein was

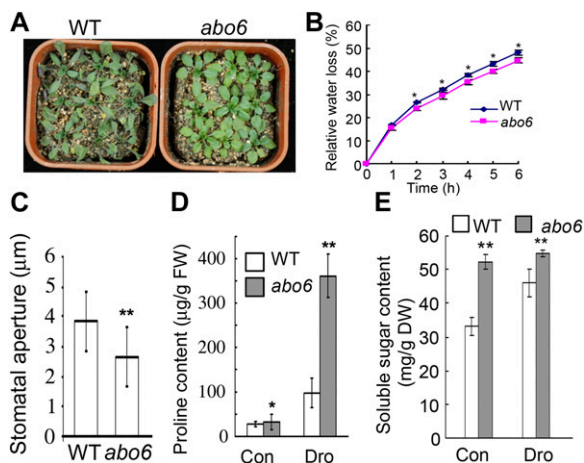


Figure 2. *abo6* Is More Drought Tolerant Than the Wild Type.

(A) Phenotypes of seedlings grown in soil and subjected to drought treatment. Seedlings were grown in soil under short-day (12 h light/12 h dark) conditions for 2 weeks before water was withheld. Seedlings were photographed after water had been withheld for 10 d. WT, the wild type.

(B) Relative water loss in detached leaves. Detached leaves from nine seedlings grown in soil under short-day conditions were weighed at the time of detachment (=100% water content or 0% water loss), kept uncovered on the greenhouse bench, and weighed each hour for 6 h. Three independent experiments were performed with the similar results. Data are means \pm SE of three biological repetitions, $n = 3$. * $P < 0.05$.

(C) Stomatal aperture of seedlings growing in soil under water sufficient conditions. At least 90 apertures in total were measured. Data are means \pm SE of three biological repetitions. ** $P < 0.01$.

(D) Pro content of seedlings grown under water-sufficient (control [Con]) and drought (Dro) conditions. FW, fresh weight.

(E) Soluble sugar content of seedlings grown under water-sufficient and drought conditions. DW, dry weight.

In (D) and (E), leaves of 4-week-old seedlings grown in soil under short-day conditions were detached and kept uncovered on the greenhouse bench. After 3 h, Pro (D) and soluble sugar (E) content in the detached leaves were measured. Three independent experiments were performed. Data are means of three biological repetitions \pm SE, $n = 3$. * $P < 0.05$; ** $P < 0.01$.

[See online article for color version of this figure.]

colocalized with the fluorescence of the MitoTracker Red, indicating that ABO6 is targeted to mitochondria (Figure 3G).

To determine the expression of ABO6, we performed quantitative RT-PCR. We found that ABO6 transcripts were more abundant in roots and flowers than in leaves and stems (Figure 3H). Interestingly, the expression of ABO6 was reduced by ABA treatment (Figure 3I), which is consistent with the public microarray data (Nakashima et al., 2009), suggesting that it has a role in the ABA response pathway.

ABO6 Affects the Splicing of Complex I Genes in Mitochondria

DEAD box RNA helicases have been implicated in a variety of RNA metabolic processes, including RNA synthesis, RNA modification, RNA cleavage, and RNA degradation (Gong et al., 2002). Because ABO6 is targeted to mitochondria, we wanted to

determine whether it participates in mitochondrial RNA metabolism. Among the nine mitochondria-encoded *nad* genes (*nad1*, *nad2*, *nad3*, *nad4*, *nad4L*, *nad5*, *nad6*, *nad7*, and *nad9*, encoding subunits of the NADH dehydrogenase [complex I]), *nad4* and *nad7* require *cis*-splicing, and *nad1*, *nad2*, and *nad5* require both *cis*- and *trans*-splicing (Unsel et al., 1997). We found that the *abo6* mutation impaired RNA splicing in *NAD1b*, *NAD1c*, *NAD2a*, *NAD2b*, *NAD4*, and *NAD5a* but not in *NAD5c* and *NAD7* (Figure 4A) or in *COX2* (a subunit of cytochrome c oxidase [complex IV]), *RPL2*, *RPS3* (encode subunits of ribosomal proteins), and *CCB452* (involved in cytochrome c biogenesis), genes that are required for splicing but not in complex I (Figure 4C). The transcripts of *NAD5c*, *NAD7*, *COX2*, *RPL2*, *RPS3*, and *CCB452* were more abundant in *abo6* than in the wild type. The high accumulation of mitochondrial transcripts is also found in other mutants, such as *slo1*, in which a PPR gene required for RNA editing of *nad4* and *nad9* is mutated. However, the reason for this is not known (Sung et al., 2010). We further used quantitative RT-PCR (qRT-PCR) to determine the effect of the *abo6* mutation on splicing sites. For *NAD1*, the splicing in all four introns was greatly reduced in *abo6*, and the transcripts of each intron were more abundant in *abo6* than in the wild type (Figure 4B). For *NAD2*, splicing was not affected in the first (*cis*-) and second (*trans*-) intron but was impaired in the third (*cis*-) and fourth (*cis*-) intron; the abundance of transcripts of the first and second introns was not changed, but the abundance of transcripts of the third and fourth introns was increased. For *NAD4*, the *cis*-splicing in all three introns was significantly reduced, and the intron expression was higher in *abo6* than in the wild type (Figure 4B). For *NAD5*, the third exon is very short and the primers were designed to cover the second and fourth exons. Both the *cis*- and *trans*-splicing (introns 2 and 3) were reduced in *NAD5*, and transcripts of the corresponding introns were increased (Figure 4B). These results indicate that ABO6 is involved in both *cis*- and *trans*-splicing of some *nad* genes. We also found that ABA treatment reduced the expression of *NAD1*, *NAD2*, and *NAD5* but had no effect on the expression of *NAD4* (Figure 4D).

ROS from Mitochondria Are the Second Messengers for ABA Inhibition of Primary Root Growth and Seed Germination in *abo6*

Impairment of complex I in mitochondria would result in respiratory dysfunction and would elicit the production of excess ROS. To detect ROS production from mitochondria, we generated transgenic *Arabidopsis* plants that harbored a mitochondrial matrix-targeted superoxide indicator, Mito-cpYFP, that emits strong fluorescence in the presence of the superoxides found in mitochondria with superoxide in mitochondria, but not with other ROS or not in other cell organelles (Wang et al., 2008). In the absence of ABA treatment, *abo6*/Mito-cpYFP emitted stronger fluorescence than the wild type/Mito-cpYFP (Figure 5A), indicating that *abo6* accumulated a higher level of ROS than the wild type. ABA treatment induced higher levels of fluorescence in both *abo6*/Mito-cpYFP and wild type/Mito-cpYFP than no ABA treatment (Figure 5A), and *abo6*/Mito-cpYFP emitted stronger fluorescence than wild type/Mito-cpYFP (Figure 5A). Quantification of intensities verified that *abo6* produced more ROS than did the wild type with

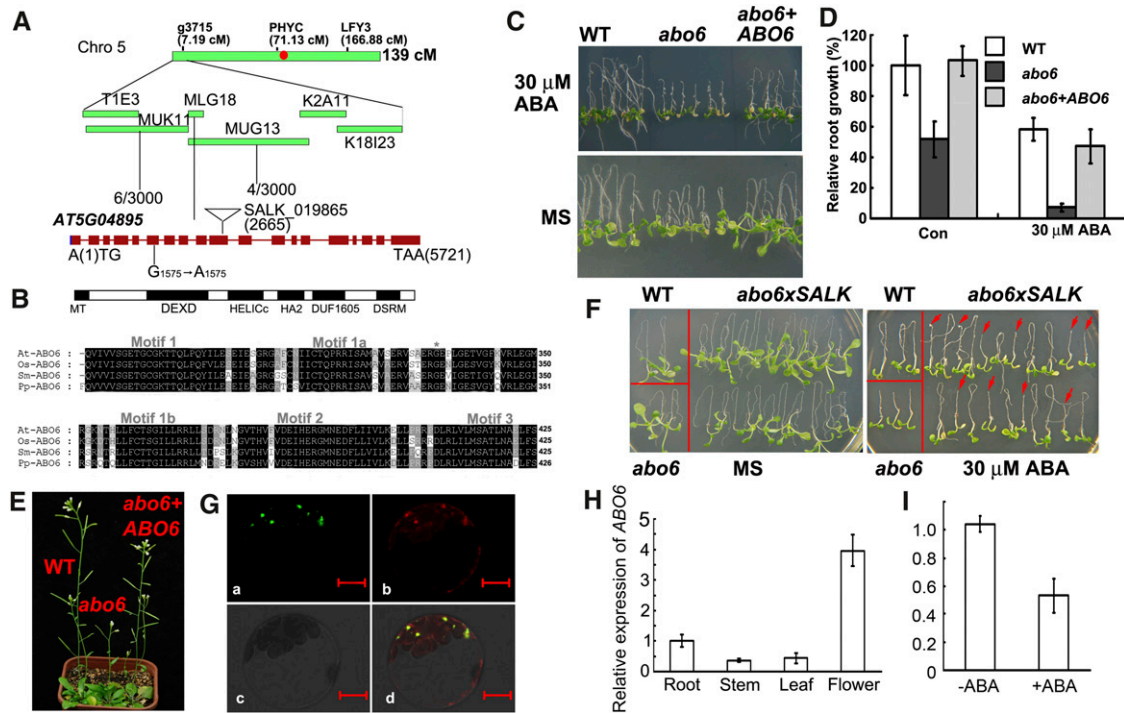


Figure 3. Cloning of *ABO6*.

(A) Map-based cloning of *ABO6*. *ABO6* was mapped to the top of chromosome 5. A total of 1500 samples were used to narrow the location of *ABO6* to BAC clones MUK11 and MUG13. A G-to-A mutation in position 1575 and a T-DNA insertion in position 2665 in AT5G04895 are indicated. Red dot, centromere; cM, centimorgans.

(B) The structure of the predicted *ABO6* protein and DEXD domain. MT, mitochondrial signal peptide; DEXD, DEXD motif; HELICc, a helicase C-terminal domain; HA2, a helicase-associated domain; DUF1605, domain-of-unknown function; DSRM, double-stranded RNA binding domain. The DEXD domains of *ABO6* homologs from *Oryza sativa* AAL58955 (Os-*ABO6*), *Selaginella moellendorffii* EFJ13473 (Sm-*ABO6*), and *Physcomitrella patens* EDQ53672 (Pp-*ABO6*) were aligned with *ABO6* using ClustalX 2.0.5, and the conserved DEXH domains was selected. The asterisk refers to the conserved amino acid Gly-334 of *ABO6* that was mutated to Glu in *abo6* in motif 1a.

(C) ABA sensitivity of *abo6* complemented with *Pro super:ABO6*. The wild type (WT), *abo6*, and transgenic line 9 (*abo6+ABO6*) were grown on MS medium containing 0 or 30 μ M ABA.

(D) Relative primary root growth (root length) of *abo6*, *abo6* complemented with *Pro super:ABO6*, and the wild type on MS medium with and without ABA. Primary root length of the wild type on MS medium without ABA was taken as 100%.

(E) Growth phenotypes of *abo6*, *abo6* complemented with *Pro super:ABO6*, and wild-type seedlings growing in soil.

(F) ABA-sensitive phenotype of F1 seedlings from *abo6* crossed with a heterozygous T-DNA line disrupting AT5G04895 (*SALK_019865*, see [A] for insertion position). Four-day-old seedlings were transferred to MS medium containing 0 or 30 μ M ABA, and seedlings were photographed 7 d later. Red arrows point to *abo6/SALK_019865*.

(G) Localization of the *ABO6* signal peptide fused with GFP. The signal peptide of *ABO6* was fused with GFP and transiently expressed in protoplasts of *Arabidopsis* leaves. The protoplasts were stained with MitoTracker Red and observed with a confocal laser microscope. (a) GFP image; (b) MitoTracker Red image; (c) bright-field images; (d) merged images of GFP and MitoTracker Red. Bars = 10 μ m.

(H) Relative expression of *ABO6* in roots, stems, leaves, and flowers as determined by qRT-PCR. *ACTIN2/8* was used as a control. Three independent experiments were performed, each with three technical replicates. Results shown are from one representative experiment.

(I) Expression of *ABO6* is reduced by ABA treatment. Seedlings were treated with 50 μ M ABA for 5 h, and total RNAs were used for qRT-PCR. *ACTIN2/8* was used as a control. Three independent experiments were performed. Data are means of three biological repetitions \pm SE, $n = 3$.

or without ABA treatment (Figure 5B). Nitroblue tetrazolium (NBT) staining (for detection of superoxides) of root tips supported these results under both normal conditions and ABA treatment (Figure 5C, also see Figures 7C, 7D, 8I, and 8J for quantification). These results indicate that ABA induces the accumulation of ROS in mitochondria, and *abo6* mutation leads to increased ROS accumulation in mitochondria.

We used 3', 3'-diaminobenzidine (DAB; for detection of H_2O_2) staining to examine ROS in leaves and found that the

concentration of ROS was higher in *abo6* leaves than in wild-type leaves (Figure 5D). ABA and drought treatment induced more ROS in *abo6* than in the wild type (Figure 5D). Similar results were obtained when we used DAB staining to measure ROS accumulation with and without ABA treatment in primary roots (Figure 5E). 2',7'-Dichlorodihydrofluorescein diacetate (DCFH-DA) staining (a fluorescent probe for detection of H_2O_2) and its quantification in primary root tips confirmed the higher accumulation of ROS in *abo6* than in the wild type with and

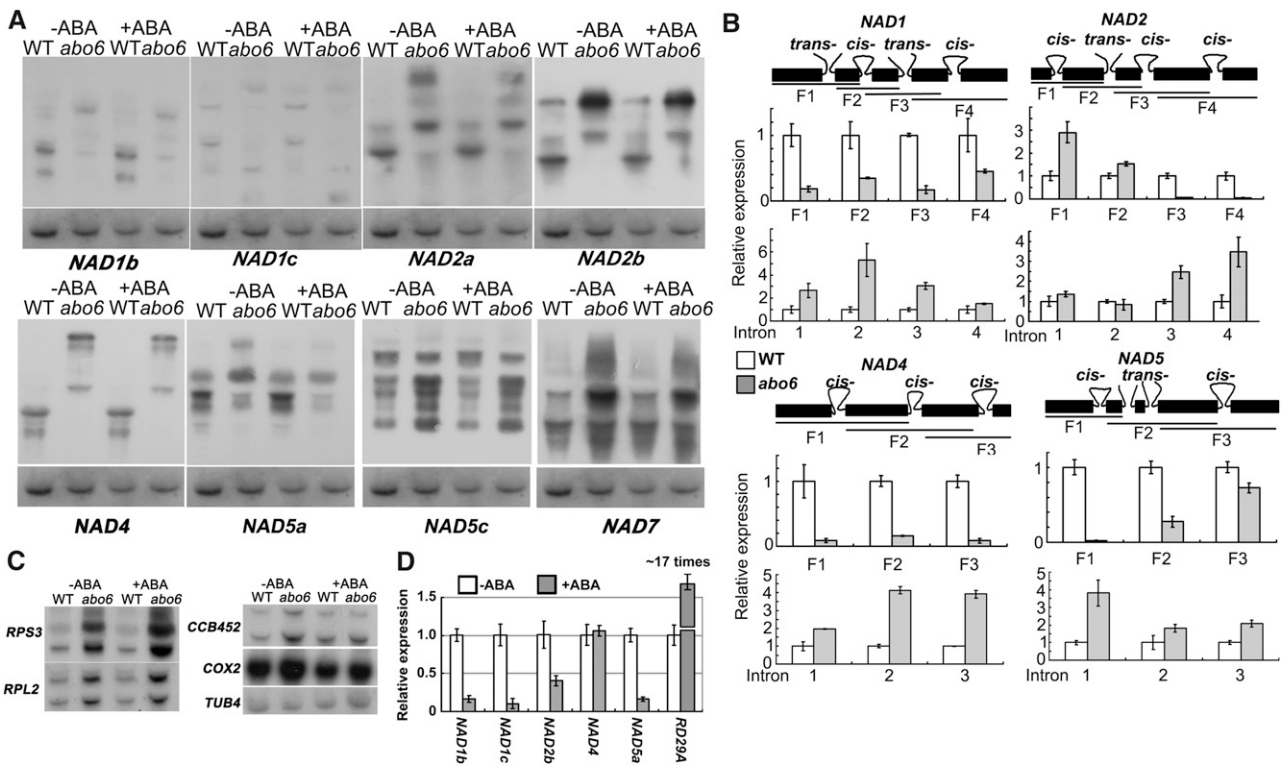


Figure 4. RNA Gel Blot of *nad* Genes.

(A) RNA gel blot analysis of the expression of *nad* genes or gene fragments using specific probes. Probes: *NAD1b*, the third exon; *NAD1c*, the fifth exon; *NAD2a*, the second exon; *NAD2b*, the fourth exon; *NAD4*, the third exon; *NAD5a*, the second exon; *NAD5c*, the fourth exon; *NAD7*, the third exon (see **[B]** for the exon fragments used). *TUBULIN4* was used as a loading control. WT, the wild type.

(B) qRT-PCR analysis of the transcripts of different exons and introns. In each gene, *trans*- or *cis*-splicing is indicated. The amplified fragment is labeled F1, F2, F3, or F4 or is indicated by intron number.

(C) RNA gel blots of *COX2* (a subunit of cytochrome c oxidase [complex IV]), *RPL2*, *RPS3* (encoding subunits of ribosomal proteins), and *CCB452* (involved in cytochrome c biogenesis) genes that are required for splicing. *TUBULIN4* was used as a loading control.

(D) qRT-PCR analysis of the transcripts of some *NAD* genes by ABA treatment. The transcripts without ABA treatment were compared with those under ABA treatment. Three independent experiments were done with similar results, each with three biological replicates. Results shown are from one representative experiment. *RD29A* was used as a positive control for effective ABA induction.

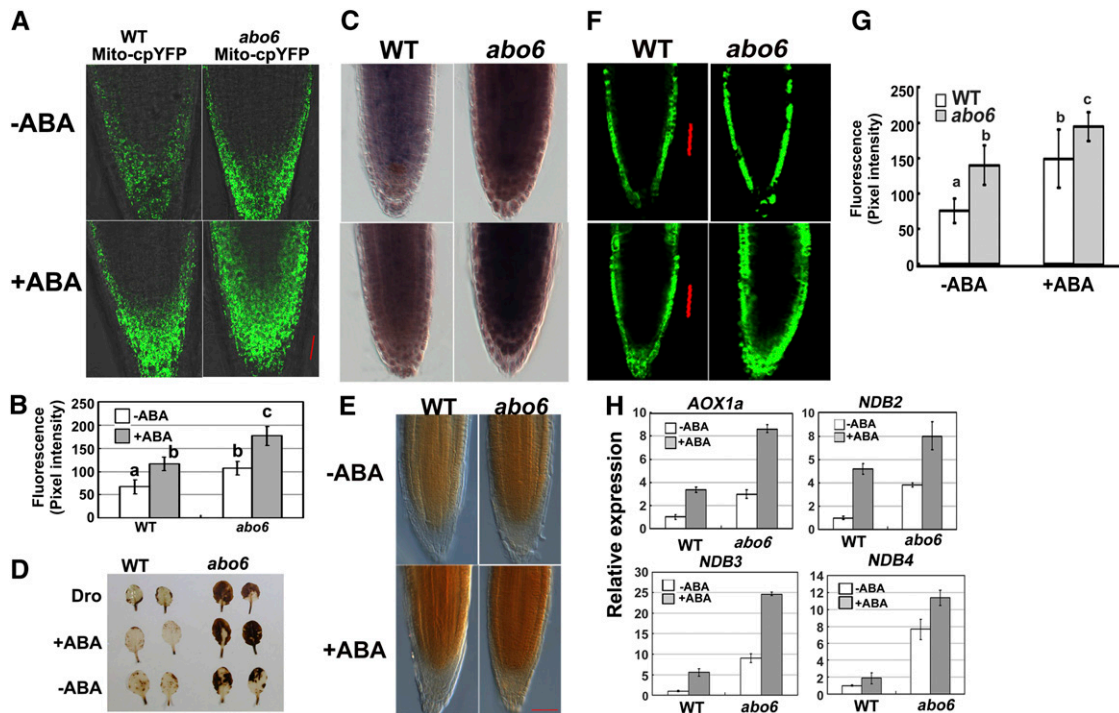
without ABA treatment (Figures 5F and 5G). These results indicate that *abo6* mutants accumulate more ROS than the wild type in both leaves and roots and that ABA treatment enhances ROS production.

ROS produced in mitochondria usually act as retrograde signals to induce the expression of some nuclear genes, including alternative oxidase and type II NAD(P)H dehydrogenases (Clifton et al., 2005). We tested the gene expression of *AOX1a* and the B class NADH dehydrogenase gene family (*NDB2*, *NDB3*, and *NDB4*) in *abo6* and the wild type. As shown in Figure 5H, the transcripts of *AOX1a*, *NDB2*, *NDB3*, and *NDB4* were several times more abundant in *abo6* than in the wild type under normal growth conditions. ABA treatment increased the transcripts of these four genes in both *abo6* and the wild type (Figure 5H).

To determine whether the ROS produced from mitochondria can act as second messengers that inhibit primary root growth, we compared the primary root growth of the *abo6* mutant with that of the wild type on MS medium supplemented with a ROS

scavenging reagent, reduced GSH. As shown in Figures 6A and 6B, relative primary root growth was similar for the wild type and *abo6* on MS medium containing 300 μ M GSH or 600 μ M GSH. As shown above, 30 μ M ABA greatly inhibited the primary root growth of *abo6*, while the relative primary root growth of *abo6* was comparable with that of the wild type on MS medium supplemented with 30 μ M ABA plus 300 μ M GSH or 600 μ M GSH. The addition of different concentrations of GSH to the medium also released the ABA inhibition of *abo6* seed germination (Figures 6C and 6D).

Previous studies suggested that a GSH pool is important for mediating plant growth (Bashandy et al., 2010; Koprivova et al., 2010a). To determine whether the response of *abo6* to GSH was specific or was representative of its response to other ROS scavenging agents, we investigated whether another ROS scavenging agent, DTT, could also recover the ABA-sensitive phenotypes of *abo6*. The addition of 300 μ M DTT did not apparently affect the primary root growth of the wild type and *abo6* but clearly released the ABA inhibition of primary root growth in both *abo6* and the wild



type and made the relative root growth of *abo6* comparable to that of the wild type (Figures 6E and 6F). The addition of 600 μ M DTT weakly inhibited primary root growth of the wild type but not of *abo6* and released the ABA inhibition of primary root growth of *abo6* and the wild type. The addition of DTT also reduced the inhibition of seed germination greening caused by ABA treatment in *abo6* (Figures 6G and 6H). We further compared two other mutants, *ndufs4* (for NADH dehydrogenase [ubiquinone] fragment S subunit 4 of complex I) and *abo5* (cis-splicing of mitochondrial *nad2* intron 3 in complex I), on MS medium supplemented with GSH or DTT. Two mutants are sensitive to ABA in seed germination and root growth (Liu et al., 2010). The addition of GSH or DTT to the MS medium released the ABA inhibition of both seed germination and primary root growth in the two mutants to a similar degree as in *abo6* (see Supplemental Figure 2 online). These results suggest that the oxidation status is important for ABA inhibition of seed germination and primary root growth.

We further tested whether a specific nontoxic inhibitor of γ -glutamylcysteine synthetases, BSO, could impact the growth of *abo6* and the wild type. The root growth of *abo6* was more resistant to BSO than that of the wild type (Figures 6I and 6J), which is consistent with other complex I defective mutants, such as *bir6* (for *BSO-insensitive roots6*), which is defective in splicing of intron 1 of the *nad7* transcript, *css1*, which is disrupted in the splicing of an intron in maturase, and a γ -carbonic anhydrase mutant (*At1g47260*) (Koprivova et al., 2010b). The resistance to BSO is consistent with the higher accumulation of GSH under BSO treatment in *abo6* than in the wild type (Figure 6K), but the mechanism explaining why complex I mutants with higher GSH are resistant to BSO is unknown (Koprivova et al., 2010b). These results suggest that at least the GSH pool in these mutants is not lower than that in the wild type under ABA or BSO treatment. Increased BSO combined with ABA had an additive effect on the inhibition of root growth in both *abo6* and the wild type (Figures

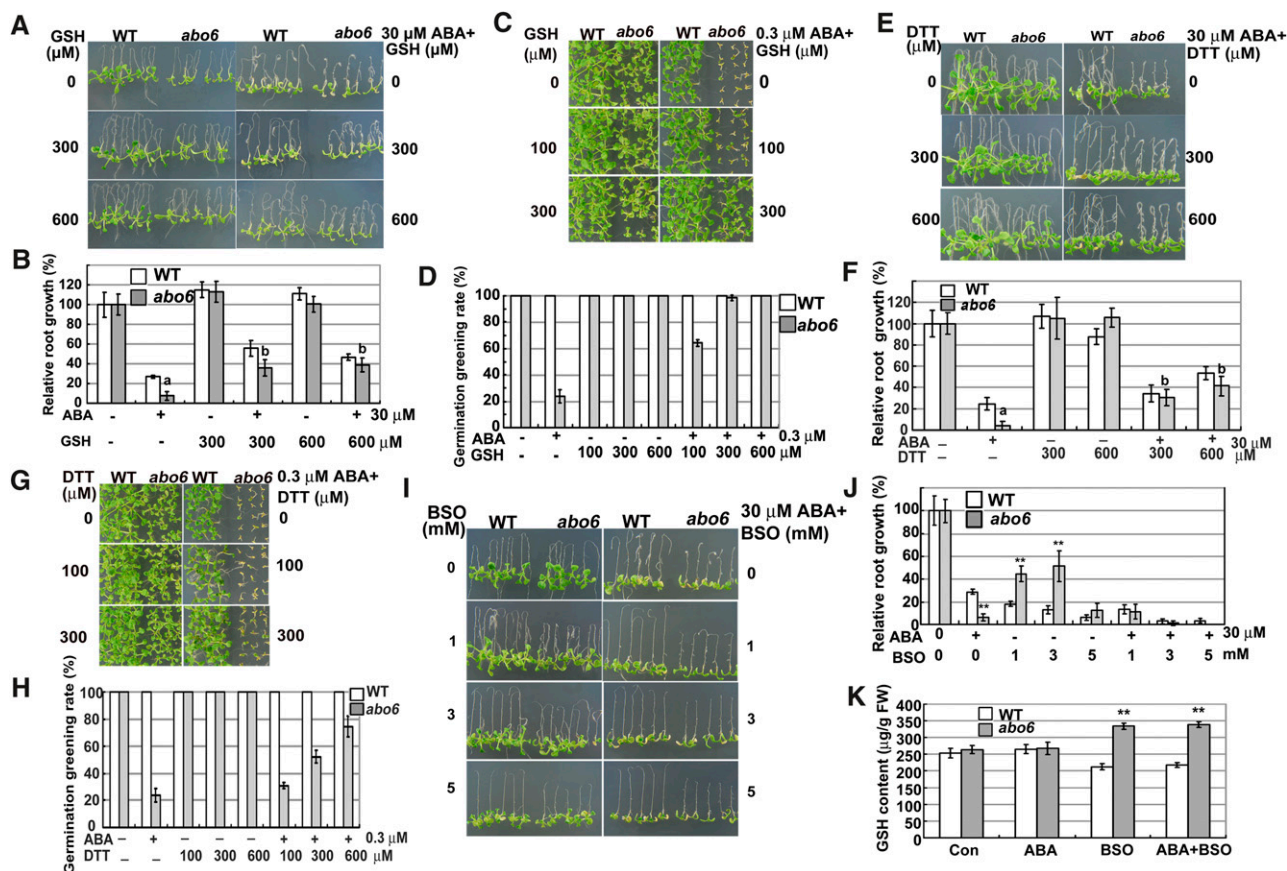


Figure 6. Exogenous Addition of GSH or DTT Can Partially Rescue the ABA-Sensitive Phenotypes of *abo6*.

(A) Primary root growth of seedlings on MS medium or MS medium containing ABA, GSH, or ABA plus GSH, respectively. Four-day-old seedlings were transferred to MS medium or MS medium containing different concentrations of GSH, ABA, or GSH plus ABA for 7 d before being photographed. WT, the wild type.

(B) Statistical analysis of relative primary root length in (A). Samples of *abo6* with different letters are significantly different: $P < 0.01$.

(C) Germination greening of seeds on MS medium or MS medium supplemented with ABA, GSH, or ABA plus GSH. Plates were kept in a growth chamber for 14 d before they were photographed.

(D) Statistical analysis of the seed germination greening rate in (C).

(E) The primary root growth of seedlings on MS medium or MS medium supplemented with ABA, DTT, or ABA plus DTT.

(F) Statistical analysis of the relative primary root length in (E). Samples of *abo6* with different letters are significantly different: $P < 0.01$.

(G) Germination greening of seeds on MS medium or MS medium supplemented with ABA, DTT, or ABA plus DTT. Plates were kept in a growth chamber for 14 d before they were photographed.

(H) Statistical analysis of seed germination greening rate in (G).

(I) Primary root growth of seedlings on MS medium or MS medium supplemented with ABA, BSO, or ABA plus BSO.

(J) Statistical analysis of relative primary root length in (I). $**P < 0.01$.

(K) GSH content in the roots of wild type and *abo6* under different treatments. $**P < 0.01$.

In (B), (F), and (J), primary root length of the wild type or *abo6* on MS alone was set at 100%. Values are means \pm SE in (B), (D), (F), (H), (J), and (K). Three independent experiments were performed, each with triple replicates (more than 30 seeds or 10 roots for each replicate).

[See online article for color version of this figure.]

6I and 6J), indicating that BSO enhancement of oxidative stress increases ABA-mediated inhibition of root growth.

Dominant-Negative Mutations in *ABI1* and *ABI2* Reduce ROS Production and Release the ABA Sensitivity of *abo6* in Root Growth

ABI1 and *ABI2* encode protein phosphatases 2C (Leung et al., 1994, 1997; Meyer et al., 1994), which are important

components in early ABA signaling. The dominant-negative mutations in *abi1-1* and *abi2-1* block the interaction of PYR/PYL/RCAR ABA receptors with *ABI1* and *ABI2*, resulting in the inhibition of ABA signal transduction (Cutler et al., 2010). In the *abi1-1* mutant, ABA-induced ROS accumulation is greatly reduced in guard cells, while in the *abi2-1* mutant, ABA-induced ROS accumulation is normal in guard cells, but the ROS signal cannot be transmitted to downstream targets to regulate stomatal movement (Murata et al., 2001). We used cpYFP

superoxide indicator to compare ROS accumulation in *abo6*, *abi1-1*, *abi2-1*, and the wild type. As shown in Figures 7A and 7B, both *abi1-1*/Mito-cpYFP and *abi2-1*/Mito-cpYFP emitted less fluorescence than *abo6*/Mito-cpYFP or wild type/Mito-cpYFP. *abo6 abi1-1*/Mito-cpYFP and *abo6 abi2-1*/Mito-cpYFP emitted more fluorescence than *abi1-1*/Mito-cpYFP or *abi2-1*/Mito-cpYFP but much less than *abo6*/Mito-cpYFP or wild type/Mito-cpYFP. ABA treatment resulted in more fluorescence than no ABA treatment in *abi1-1*/Mito-cpYFP, *abi2-1*/Mito-cpYFP, *abo6 abi1-1*/Mito-cpYFP, or *abo6 abi2-1*/Mito-cpYFP plants. NBT staining of root tips confirmed these results, both under normal conditions and ABA treatment (Figures 7C and 7D). Because *abi1-1* and *abi2-1* are in the Landsberg *erecta* (*Ler*) accession, we also included *Ler* in our analysis. The primary roots of *Ler* produced more ROS than those of Columbia *gl1* (here used as the wild-type control) (Figures 7C and 7D), which might partially explain the greater ABA sensitivity of *Ler* than Columbia in both seed germination greening and primary root growth.

Next, we performed both DAB and DCFH-DA staining to analyze ROS (H_2O_2) production. Both *abi1-1* and *abi2-1* accumulated less ROS (H_2O_2) in roots than the wild type under ABA treatment or no ABA treatment (Figures 7E and 7F for DAB staining and Figures 7G and 7H for DCFH-DA), suggesting that ROS production regulated by ABI2 in roots is different from that in guard cells (Murata et al., 2001). ABA treatment increased ROS accumulation in all plants. The *abi1-1 abo6* and *abi2-1 abo6* double mutants produced more ROS than *abi1-1* or *abi2-1*, respectively, which all accumulated less ROS than the wild type or *abo6* under ABA treatment or no ABA treatment. The primary roots of *Ler* accumulated more H_2O_2 than those of Columbia.

The *abi1-1 abo6* and *abi2-1 abo6* mutants were resistant to ABA inhibition of primary root growth and seed germination greening (see Supplemental Figure 3 online), which was not caused by a change in the accumulation of GSH in roots (see Supplemental Figure 4 online). As previous studies have indicated that ABA regulates ROS production at the plasma membrane (Kim et al., 2010), our results suggest that the early ABA signaling components, ABI1 and ABI2, also regulate ROS production from mitochondria.

ABA-Mediated Inhibition of *abo6* Primary Root Growth Is Alleviated by the *rbohF* Mutation

The *Arabidopsis* genome contains 10 NADPH oxidase catalytic subunit genes. A previous study indicated that ABA evaluates ROS production by regulating the plasma membrane NADPH oxidases RBOHD and RBOHF (Kwak et al., 2003). To determine the contribution of the mitochondrial ROS made by *abo6* to the cellular response, we performed a phenotypic analysis of *abo6* and the *rbohF* mutant, which is insensitive to ABA in terms of primary root growth (Kwak et al., 2003). *abo6 rbohF* showed similar ABA sensitivity as *abo6* in terms of seed germination, indicating that *abo6* dominates the seed germination (Figures 8A and 8B). The primary root growth of *abo6 rbohF* was faster than that of *abo6* but slower than the wild type and *rbohF* under normal conditions (Figures 8C and 8D). The primary root growth

of *abo6 rbohF* was less inhibited by ABA than was *abo6* (Figures 8E and 8F), indicating that the *rbohF* mutant could alleviate the ABA inhibition of primary root growth of *abo6*. Under both ABA and no ABA treatment, *rbohF* accumulated similar levels of superoxide in mitochondria as the wild type, as detected by Mito-cpYFP fluorescence (Figures 8G and 8H). *abo6 rbohF* accumulated a similar level of superoxides in mitochondria as *abo6* in normal conditions and less than *abo6* upon ABA treatment (Figures 8G and 8H). These results indicate that RBOHF affects superoxide accumulation in mitochondria under ABA treatment. NBT staining showed similar superoxide accumulation patterns as Mito-cpYFP fluorescence (Figures 8I and 8J). Upon DAB staining (Figures 8K and 8L), *rbohF* accumulated less H_2O_2 in root tips than the wild type in both the presence and absence of exogenously applied ABA, while *abo6 rbohF* accumulated similar levels of H_2O_2 as *abo6* in the absence of ABA treatment, less than *abo6* under ABA treatment, more than *rbohF* in both the presence and absence of ABA treatment, more than the wild type under normal conditions, and similar as the wild type under ABA treatment. DCFH-DA staining (Figures 8M and 8N) and showed similar H_2O_2 accumulation patterns in all phenotypes as DAB staining. Taken together, these results suggest that ROS homeostasis can be affected by the ROS produced at both the plasma membrane and mitochondria in *Arabidopsis*.

ProDR5:GUS and *ProIAA2:GUS* Expression Are Reduced in the Primary Root Tips of *abo6*

DR5 is a synthetic promoter that contains an auxin response element whose expression provides reliable information concerning auxin distribution in roots and other tissues (Ulmasov et al., 1997; Benková et al., 2003). We introduced *ProDR5:GUS* (for synthetic auxin response element D1-4 with site-directed mutants in the 5'-end from soybean: β -glucuronidase) into the *abo6* mutant. GUS staining in the cotyledon was less in *abo6* than in the wild type. In the primary root tips, GUS staining was faint in *abo6* but strong in the wild type (Figure 9A). ABA treatment reduced *ProDR5:GUS* expression in both primary root tips and leaves of the wild type and also in leaves of *abo6* (Figure 9A). The addition of 1-naphthalene acetic acid (NAA) to the medium induced the expression of GUS to higher levels in both *abo6* and the wild type (Figure 9B), indicating that the auxin signaling pathway is not defective in *abo6*. However, *ProDR5:GUS* expression in *abo6* was still lower than that in the wild type upon NAA treatment, suggesting that ROS are negative regulators of auxin response (Nakagami et al., 2006). *IAA2* is another auxin marker whose expression is rapidly induced by auxin (Shibasaki et al., 2009). We introduced *Indole-3-acetic acid inducible2 (ProIAA2):GUS* into the *abo6* mutant. The expression of *ProIAA2:GUS* in primary root tips was lower in *abo6* than in the wild type (Figure 9C). ABA treatment (30 μ M) reduced *ProIAA2:GUS* expression in both *abo6* and the wild type. As a previous study indicates that a low concentration of ABA (2 μ M) likely increases *ProIAA2:GUS* expression (Belin et al., 2009), we performed similar experiments to test the effect of ABA treatment on *ProIAA2:GUS* expression. As shown in Figure 9D, GUS staining was greatly reduced by ABA treatment when staining was performed for a short time (40 min). When samples were

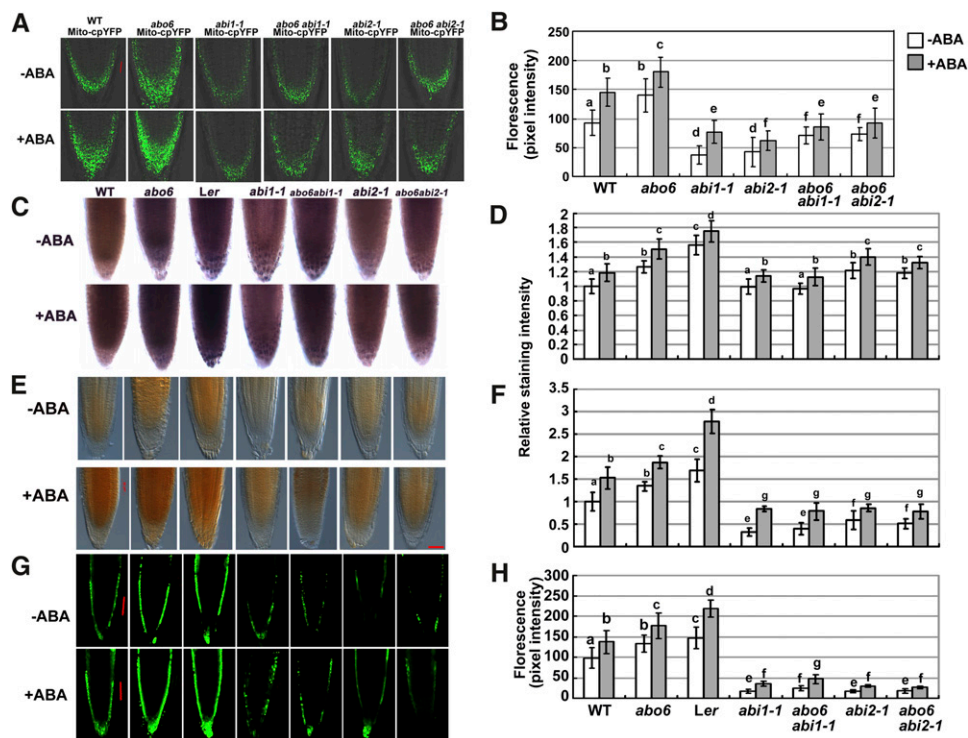


Figure 7. Genetic Analysis of *abo6* with *abi1-1* and *abi2-1*.

(A) Fluorescence analysis of mitochondrial cpYFP in the roots of *abo6*, *abi1-1*, *abi2-1*, *abo6 abi1-1*, *abo6 abi2-1*, and wild-type (WT) plants without or with ABA treatment. Bar = 50 μ m.

(B) Intensity of Mito-cpYFP fluorescence quantified using AxioVision Rel. 4.8 software. About 20 roots were analyzed for each experiment. Values are means \pm SE of three biological repetitions. Samples with different letters are significantly different: $P < 0.05$.

(C) NBT staining (detection of superoxides) of root tips of the wild type (Columbia), *abo6*, *Ler*, *abi1-1*, *abi2-1*, *abo6 abi1-1*, and *abo6 abi2-1* under both normal conditions and ABA treatment.

(D) Relative intensity of NBT staining in (C). About 20 roots were analyzed for each experiment. Values are means \pm SE of three biological repetitions. Samples with different letters are significantly different: $P < 0.05$.

(E) DAB staining of the primary roots of the wild type, *abo6*, *Ler*, *abi1-1*, *abi2-1*, *abo6 abi1-1*, and *abo6 abi2-1* plants treated or not with 30 μ M ABA for 5 h. Bar = 50 μ m.

(F) Relative intensity of DAB staining in (E). About 20 roots were analyzed for each experiment. Values are means \pm SE of three biological repetitions. Samples with different letters are significantly different: $P < 0.05$.

(G) DCFH-DA staining assay of the primary roots in *abo6*, wild-type, *Ler*, *abi1-1*, *abi2-1*, *abo6 abi1-1*, and *abo6 abi2-1* plants treated or not with 30 μ M ABA for 5 h. Bar = 50 μ m.

(H) Intensity of DCFH-DA staining quantified using AxioVision Rel. 4.8 software. About 20 roots were analyzed for each experiment. Values are means \pm SE of three biological repetitions. Samples with different letters are significantly different: $P < 0.05$.

stained for a longer period (180 min), the strength of GUS staining was hard to compare, suggesting that the conditions used by our lab and by Belin et al. (2009) might have differed. These results suggest that auxin accumulation or responsiveness is less in *abo6* than in the wild type.

Exogenous Auxins Restore the ABA Inhibition of Seed Germination Greening and Primary Root Growth of *abo6*

Previous studies indicate that ROS degrade or oxidize auxin and that ROS are negative regulators of the auxin response (Gazarian et al., 1998; Nakagami et al., 2006). The high accumulation of ROS in *abo6* may perturb auxin homeostasis and thereby affect root growth. We tested whether the exogenous

addition of auxins could restore the ABA sensitivity of *abo6*. The two auxins used were NAA, which is able to cross the plasma membrane without the help of auxin facilitators, and 2,4-D, which requires auxin facilitators to cross the plasma membrane. Wild-type seeds germinated earlier in the presence of 0.3 nM 2,4-D or 0.3 nM NAA than in the absence of 2,4-D or NAA (Figures 10A and 10B), and the addition of 0.3 nM 2,4-D or 0.3 nM NAA could release the ABA-mediated inhibition of seed germination of the wild type (Figure 10C), indicating that auxin is able to promote seed germination of wild-type *Arabidopsis*. An increase from 0.03 to 3 nM NAA or 2,4-D to the medium restored the ABA-mediated inhibition of seed germination greening of *abo6* (Figures 10D to 10G). Similarly, the addition of low concentrations of NAA or 2,4-D to the medium also

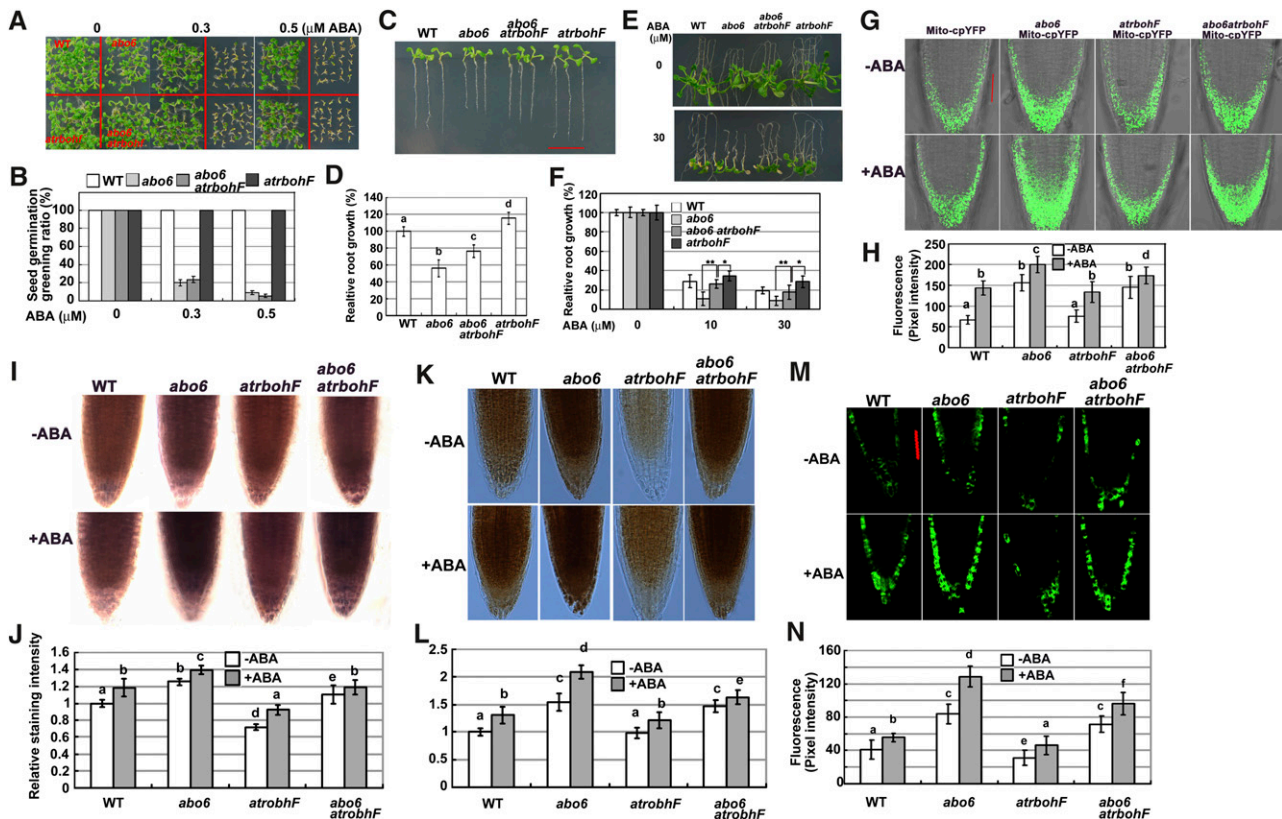


Figure 8. ABA Inhibition of Primary Root Growth of *abo6* Can Be Compromised by the *rbohF* Mutation.

(A) and (B) Seed germination greening of the wild type (WT), *abo6*, *rbohF*, and *abo6 rbohF* on MS medium containing different concentrations of ABA. About 30 seeds were counted in each of three plates for one experiment, and three independent experiments were performed with similar results in (B). Data are means \pm SE of three biological repetitions.

(C) and (D) Root growth comparison of the wild type, *abo6*, *rbohF*, and *abo6 rbohF* (7-d-old seedlings) on MS medium. Three independent experiments were performed, each with triple replicates (more than 10 roots for each replicate) in (D). Samples with different letters are significantly different: $P < 0.01$. (E) and (F) ABA inhibition of primary root growth in wild-type, *abo6*, *rbohF*, and *abo6 rbohF* seedlings. Four-day-old seedlings were transferred to MS medium containing different concentrations of ABA and grown for 14 d. Primary root length of the wild type or *abo6* on MS alone was set at 100%. Three independent experiments were performed, each with triple replicates (more than 10 roots for each replicate). * $P < 0.05$; ** $P < 0.01$.

(G) Fluorescence analysis of mitochondrial cpYFP in the roots of wild-type, *abo6*, *rbohF*, and *abo6 rbohF* plants treated or not with 50 μ M ABA for 5 h. (H) Intensity of Mito-cpYFP quantified using AxioVision Rel. 4.8 software. About 20 roots were analyzed for each experiment. Values are means \pm SE of three biological repetitions. Samples with different letters are significantly different: $P < 0.05$ (b and d) or 0.01.

(I) NBT staining of root tips of wild-type, *abo6*, *rbohF*, and *abo6 rbohF* plants treated or not with 50 μ M ABA for 5 h. (J) Relative intensity of NBT staining in (I). About 20 roots were analyzed for each experiment. Values are means \pm SE of three biological repetitions. Samples with different letters are significantly different: $P < 0.05$.

(K) DAB staining assay of the primary roots in the wild type *abo6*, *rbohF*, and *abo6 rbohF* treated or not with 50 μ M ABA for 5 h. Bar = 50 μ m.

(L) Relative intensity of DAB staining in (K). About 20 roots were analyzed for each experiment. Values are means \pm SE of three biological repetitions. Samples with different letters are significantly different: $P < 0.05$.

(M) DCFH-DA staining of the primary roots of wild-type, *abo6*, *rbohF*, and *abo6 rbohF* plants treated or not with 50 μ M ABA for 5 h. Bar = 50 μ m.

(N) Fluorescence intensity of DCFH-DA staining quantified using AxioVision Rel. 4.8 software. About 20 roots were analyzed for each experiment. Values are means \pm SE of three biological repetitions. Samples with different letters are significantly different: $P < 0.05$.

released the inhibition of primary root growth by 30 μ M ABA in *abo6* (Figures 10H to 10K).

The Expression of Auxin Carriers Is Less in *abo6* Than in the Wild Type

The expression of auxin transport proteins is regulated by auxin homeostasis. The reduced auxin response in *abo6* may be due

to perturbed polarized auxin transport, reduced auxin levels, or both. We compared the expression of auxin transport proteins using *PIN-FORMED1* (*PIN1*), *PIN2*, or *AUXIN RESISTANT1* (*AUX1*) promoter-derived *PIN1*-GFP, *PIN2*-GFP, or *AUX1*-YFP in *abo6* and the wild type. As shown in Figures 11A and 11B, the *PIN1*-GFP level was lower in *abo6* than in the wild type. ABA treatment reduced *PIN1*-GFP in both *abo6* and the wild type, but the relative level of *PIN1*-GFP was reduced more in *abo6* than in

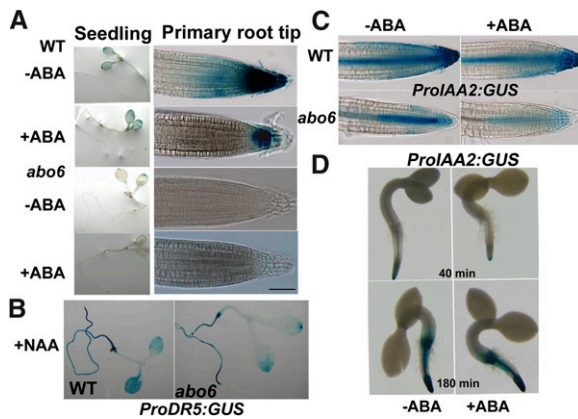


Figure 9. *abo6* Reduces Auxin Accumulation or the Auxin Signal.

- (A)** *ProDR5:GUS* expression in *abo6* and the wild type (WT). Four-day-old seedlings were transferred to MS medium with or without 30 μ M ABA for 2 d and were then stained for 24 h before being photographed. Bar = 100 μ m.
- (B)** Exogenous addition of NAA restores the expression of *ProDR5:GUS* in *abo6*.
- (C)** *ProIAA2:GUS* expression in *abo6* and the wild type. Four-day-old seedlings were transferred to MS medium with or without 30 μ M ABA for 2 d and were then stained for 40 min before being photographed.
- (D)** Comparison of *ProIAA2:GUS* expression in the wild type for different staining times without or with 2 μ M ABA treatment. Upon endosperm rupture (after \sim 36 h on MS medium at 22°C), wild-type seeds harboring *ProIAA2:GUS* were transferred to MS medium with or without 2 μ M ABA for 10 h and stained for 40 min or (180 min) before being photographed.

the wild type. Similar differences were observed between *ProPIN2:PIN2-GFP* and *ProAUX1:AUX1-YFP* roots of *abo6* and the wild type (Figures 11C to 11F). The addition of GSH to the medium increased the relative levels of PIN1-GFP, PIN2-GFP, or AUX1-YFP more in *abo6* than in the wild type (Figures 11A to 11F). The addition of BSO to the medium consistently decreased the relative amount of PIN1-GFP, PIN2-GFP, or AUX1-YFP in both *abo6* and the wild type (Figures 11A to 11F). The addition of GSH recovered the relative amount of PIN1-GFP, PIN2-GFP, or AUX1-YFP in both ABA-treated *abo6* and ABA-treated wild-type plants. However, a combination of ABA and BSO substantially decreased the amount of PIN1-GFP, PIN2-GFP, or AUX1-YFP so that the GFP/YFP signals were hardly detectably (Figure 11). These results suggest that ROS production in *abo6* contributes to the decreased abundance of auxin transport proteins, which would decrease the auxin transport capacities and auxin levels.

DISCUSSION

It has been well documented that ROS can be enhanced when plants are exposed to various abiotic stresses, such as drought and salt stress, indicating that plants have developed efficient defense systems against oxidative stress. Drought stress quickly induces the accumulation of the phytohormone ABA, which plays crucial roles in regulating stomatal movement and in modulating the expression of stress-inducible genes. ABA

stimulates the production of ROS by activating plasma membrane-localized NADPH oxidases (Kwak et al., 2003; Zhang et al., 2009), but the roles of ROS from mitochondria in the ABA signaling pathway are not well understood. Here, we provide evidence that *ABO6* encodes a mitochondria-localized DEXH RNA helicase that is involved in both *trans*- and *cis*-splicing of several, but not all, *nad* genes in mitochondrial complex I. Impairment of *ABO6* leads to increased oxidative stress in mitochondria, which is further enhanced by ABA treatment.

In plant mitochondria, the electron transfer system consists of four complexes, including NADH dehydrogenase (complex I), succinate dehydrogenase (complex II), cytochrome bc1 (complex III), and cytochrome c oxidase (complex IV). Complex I consists of more than 35 proteins encoded by both nuclear and mitochondrial DNA. Complex I is not essential in plants because plant mitochondria have four additional NAD(P)H dehydrogenases and an alternative oxidase that could bypass complex I, III, and IV. Some mutants defective in complex I, such as *Arabidopsis fro1* (Lee et al., 2002) and tobacco (*Nicotiana tabacum*) CMS I and II (Gutierrez et al., 1997), are not lethal. However, *ABO6* is an essential gene, suggesting that besides having roles in intron splicing of *nad* genes in complex I, *ABO6* may have other unidentified roles in RNA metabolism.

The *abo6* mutant exhibits various ABA-sensitive phenotypes (i.e., exposure of *abo6* to increased levels of ABA reduces seed germination, primary root growth, and stomatal opening). Interestingly, the expression of *ABO6* is downregulated by ABA treatment, suggesting that ABA modulates ROS production partially by regulating *ABO6* expression. However, we could not detect the splicing changes of *nad* genes under ABA treatment, suggesting that the reduction in *ABO6* by ABA treatment might have some undetectable effects on *nad* genes. Blocking earlier steps in the ABA signaling pathway by two dominant-negative regulators, *abi1-1* and *abi2-1*, also blocks ROS production in the mitochondria of the *abo6* mutant, indicating that ROS produced from mitochondria are regulated by the ABA signaling pathway. These results suggest that mitochondria are key players in ROS homeostasis through ABA-mediated ROS production. The results also indicate that production of ROS by mitochondria may contribute to plant adaptation to drought stress and is important in the ABA signaling pathway.

abo6 accumulated more ROS than the wild type with and without ABA treatment, suggesting that *abo6* suffers from constitutive oxidative stress. When the ROS scavenging reagent GSH was added to the growth medium to reduce ROS, the ABA-sensitive phenotypes of *abo6* were recovered to a level similar to that of the wild type. Previous studies indicate that a defect of complex I in *bir6* (encoding a PPR protein for splicing of intron 1 of *nad7*) and *css1* (impaired in intron maturase for *nad4* splicing) leads to resistance to the GSH biosynthesis inhibitor BSO (Koprivova et al., 2010b). *abo6* exhibits similar resistance as *bir6* and *css1* to BSO in terms of root growth. These results suggest that complex I mutants maintain higher GSH levels under BSO treatment. A similar result was observed in cell cultures treated with the complex I inhibitor rotenone (Garmier et al., 2008). These results indicate that impairment of complex I enhances ROS production, which in turn increases the GSH levels for antioxidation so that cellular redox homeostasis is maintained.

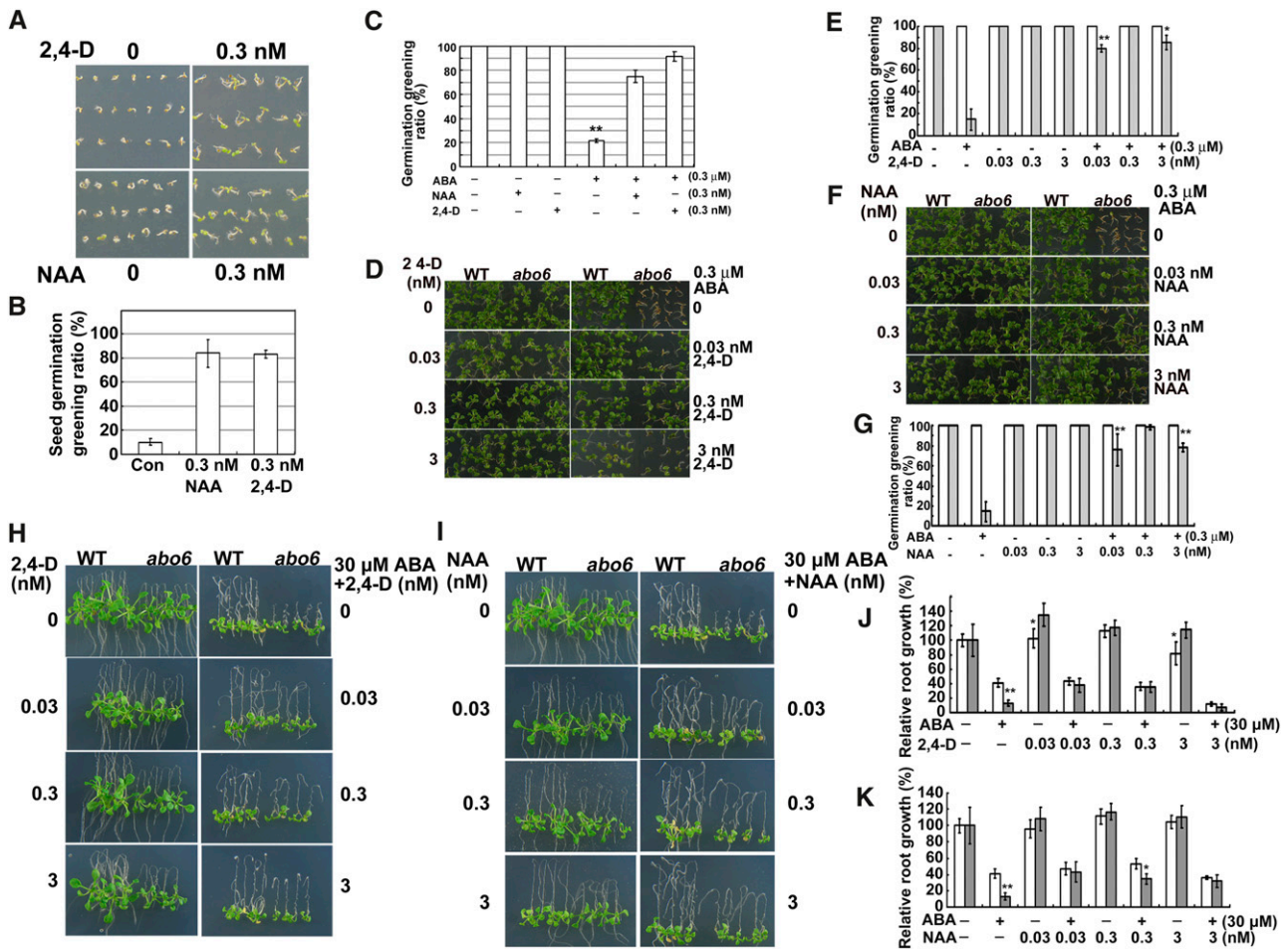


Figure 10. Auxins Promote Seed Germination and Restore ABA-Inhibited Primary Root Growth.

(A) 2,4-D and NAA promote seed germination of the wild type. Wild-type seeds were germinated on MS medium supplemented with 0.3 nM NAA or 2,4-D and kept in a growth chamber for 3 days before being photographed.

(B) Seed germination greening ratio in **(A)**. Con, MS medium.

(C) 2,4-D and NAA release the ABA-inhibited seed germination of the wild type. Wild-type seeds were germinated on MS medium supplemented with 0.3 nM 2,4-D or NAA, plus 0.3 μ M ABA and kept in a growth chamber for 5 d. Seed germination greening was quantified.

(D) Germination greening of seeds on MS medium or MS medium supplemented with ABA, 2,4-D, or ABA plus 2,4-D. Plates were kept in a growth chamber for 14 d before being photographed. WT, the wild type.

(E) Statistical analysis of seed germination greening in **(D)**.

(F) Germination greening of seeds on MS medium or MS medium supplemented with ABA, NAA, or ABA plus NAA. Plates were kept in a growth chamber for 14 d before being photographed.

(G) Statistical analysis of the seed germination greening in **(F)**.

(H) Primary root growth of seedlings on MS medium or MS medium supplemented with ABA, 2,4-D, or ABA plus 2,4-D. Four-day-old seedlings were transferred to MS medium containing 0 to 3 nM 2,4-D, ABA, or 2,4-D plus ABA for 7 d before being photographed.

(I) Primary root growth of seedlings on MS medium or MS medium supplemented with ABA, NAA, or ABA plus NAA. Four-day-old seedlings were transferred to MS medium containing 0 to 3 nM NAA, ABA, or NAA plus ABA for 7 d before being photographed.

(J) Statistical analysis of relative primary root length in **(H)**.

(K) Statistical analysis of the relative primary root length in **(I)**.

In **(B)**, **(C)**, **(E)**, **(G)**, **(J)**, and **(K)**, germination greening or primary root length of the wild type or *abo6* on MS alone was set at 100%. For statistical analysis, three independent experiments were performed, each with triple replicates (more than 30 seeds or 10 roots for each replicate). Values are means \pm SE, $n = 3$. * $P < 0.05$; ** $P < 0.01$. In **(E)**, **(G)**, **(J)**, and **(K)**, the white column is the wild type and the gray column is *abo6*.

[See online article for color version of this figure.]

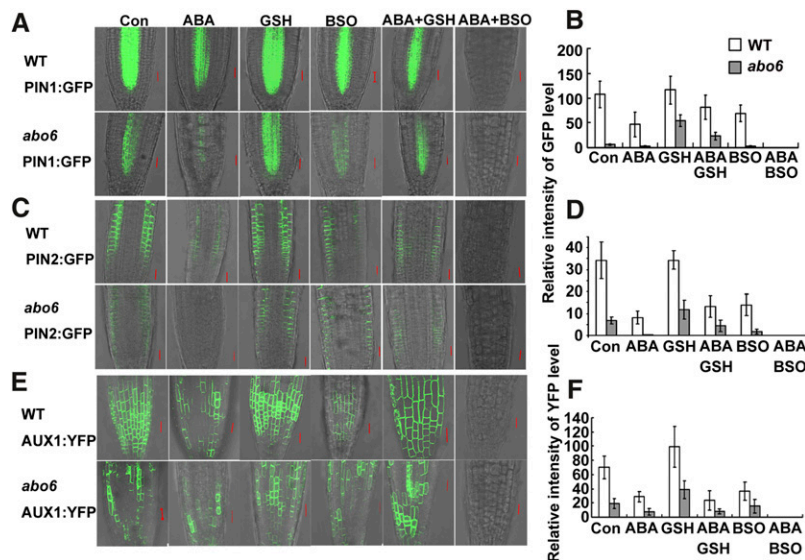


Figure 11. The Expression of PIN1, PIN2, and AUX1 in *abo6* and the Wild Type under Different Treatments.

Four-day-old seedlings were transferred to MS medium (Con) or MS medium containing 30 μ M ABA, 600 μ M GSH, 2.5 mM BSO, 30 μ M ABA plus 600 μ M GSH, or 30 μ M ABA plus 2.5 mM BSO for 2 d before being photographed with a confocal microscope with the same settings. GFP/YFP signal strength was quantified using AxioVision Rel. 4.8 software. At least 20 roots were analyzed. Values are means \pm SE. WT, the wild type. Bar = 20 μ m.

(A) *ProPIN1:PIN1-GFP* expression.

(B) Statistical analysis of GFP signal strength in (A).

(C) *ProPIN2:PIN2-GFP* expression.

(D) Statistical analysis of GFP signal strength in (C).

(E) *ProAUX1:AUX1-YFP* expression.

(F) Statistical analysis of YFP signal strength in (E).

Because of the high ROS levels in *abo6*, addition of GSH or DTT can restore the ABA sensitivity in both seed germination and primary root growth by reducing ROS accumulation. Previous studies indicate that GSH is an important regulator of root growth because a mutation of γ -glutamylcysteine synthetase in the root meristemless (*ml1*) mutant leads to root growth arrest (Vernoux et al., 2000). Although ROS is required for root growth (Foreman et al., 2003; Kwak et al., 2003), overaccumulation of ROS by ABA treatment of *abo6* inhibits seed germination and primary root growth.

We found that the expression of two auxin-responsive marker genes, *ProDR5:GUS* and *ProIAA2:GUS*, was greatly reduced by *abo6* mutation even under normal conditions. Exogenous addition of both NAA and 2,4-D restored the ABA-sensitive phenotype of *abo6*. The high accumulation of ROS in *abo6* should be the main cause of low auxin contents because auxin can be degraded or oxidized by ROS in plant cells (Gazarian et al., 1998). Furthermore, the interaction between ROS and auxin has been suggested by studies of auxin homeostasis and auxin-inducible gene regulation through increased H_2O_2 levels (Nakagami et al., 2006; Potters et al., 2007). We also observed that the auxin facilitators PIN1, PIN2, and AUX1 are more reduced in *abo6* than in the wild type by ABA treatment. Because 2,4-D but not NAA requires auxin carriers to pass through the membrane but both auxins had similar effects on ABA inhibition of seed germination and primary root growth, auxin carriers are not required for the response of *abo6* to ABA. These results suggest that reduced auxin content is the most

likely explanation for the ABA-sensitive phenotype in *abo6*. However, reduced auxin carriers might also contribute to the ABA-sensitive phenotype of *abo6* because auxin transport and auxin metabolism have feedback control (Benjamins and Scheres, 2008). Based on these results, we suspect that a reduction in both auxin content and auxin carriers contributes to the effects of ABA-mediated ROS production on the seed germination and primary root growth. The auxin-responsive phenotypes of *abo6* by overaccumulation of ROS are consistent with those observed in the *ntra ntrb cad2* triple mutants that are deficient in cytosolic NADPH thioredoxin reductases (NTRA and NTRB) and glutathione biosynthesis (CAD2) (Bashandy et al., 2010). These results demonstrate that either reducing GSH or increasing ROS will disrupt the redox homeostasis that is important for auxin transport and auxin homeostasis in the regulation of seed germination and root growth.

Crosstalk between ABA and auxin has been suggested by several studies. A study of ABA-potentiating auxin-mediated repression of embryonic axis elongation suggests that ABA enhances auxin signaling rather than increasing auxin flow or auxin levels (Belin et al., 2009). The auxin signaling-defective mutants *axr1* and *axr2* have reduced sensitivity to ABA during root elongation (Wilson et al., 1990; Tiryaki and Staswick, 2002; Monroe-Augustus et al., 2003). In another study, transgenic plants overexpressing the H_2O_2 -inducible gene *UGT74E2*, which encodes an indole-3-butyric acid (IBA) glucosyltransferase, had elevated levels of both IBA-Glc and free IBA (IAA precursor) and

a modified IAA pattern (Tsukagoshi et al., 2010); the transgenic plants exhibited enhanced ABA sensitivity, which was further enhanced by adding IBA, IBA-Glc, or IAA. Auxin can also enhance ABA inhibition of seed germination (Brady et al., 2003; Liu et al., 2007). Mutations in *INDOLE-3-BUTYRIC ACID RESPONSE5* dual specificity phosphatase and *RCN1* protein phosphatase 2A lead to auxin insensitivity but also to ABA insensitivity in germination and root growth. These studies highlight coenhancement between ABA and auxin signaling or auxin homeostasis during germination and seedling development (Liu et al., 2007; Belin et al., 2009; Tognetti et al., 2010). However, our results demonstrate that *abo6* is sensitive to ABA mainly because of the reduced auxin levels caused by ROS overproduction. Because auxin is necessary for primary root elongation, the addition of auxin complements the lack of auxin in the primary root tips and releases the ABA inhibition of primary root growth. We also showed that low concentrations of auxin promote seed germination, while other researchers showed that high concentrations of auxin do not affect seed germination (Brady et al., 2003). Seed germination of *abo6* is delayed and more sensitive to ABA than seed germination of the wild type; however, these responses of *abo6* can be reversed by the addition of low concentrations of auxin to the medium. These results indicate that a certain threshold level of auxin determines whether auxin will enhance or reduce ABA signaling and that crosstalk between ABA and auxin is complex.

METHODS

Plant Materials and Growth Conditions

Arabidopsis thaliana ecotype Columbia (*gl1*) seeds were germinated and grown on MS medium (M5519; Sigma-Aldrich) with 3% (w/v) Suc and 0.8% agar in glass plates in a light homoeothermic incubator (22°C) with 23 h light/1 h dark. For the root-bending assay, 4-d-old seedlings were moved to MS medium containing ABA, GSH, BSO, or other chemicals as indicated. For germination, ~30 seeds were placed on MS medium containing different concentrations of ABA, NaCl, mannitol, GSH, and other reagents, with three plates for each treatment. The seedlings were grown in forest soil and vermiculite (1:1) under 50 $\mu\text{mol m}^{-2} \text{s}^{-1}$ light at 22°C and 16 h light/8 h dark in a greenhouse.

Mutant Screening

The M2 ethyl methanesulfonate-mutagenized seeds of *gl1* were used for screening ABA-sensitive mutants by the root-bending assay (Yin et al., 2009) because growth of *gl1* did not differ on MS and MS supplemented with 30 μM ABA. Seedlings (4 d old) were transferred onto MS agar medium supplemented with 30 μM ABA and grown with the roots pointing upward for an additional 7 d; putative mutants with inhibited root growth were selected. The root growth phenotypes of putative mutant seedlings were rechecked in the second and third generations. Approximately 30,000 ethyl methanesulfonate-mutated M2 seedlings were screened, and one *abo6* mutant allele was obtained.

Drought Treatments, Water Loss Assay, Stomatal Aperture Measurement, and Pro and Carbohydrate Analyses

Plants grown under short-day conditions (12 h light/12 h dark) were used in these analyses. For drought treatment, 7-d-old mutant and wild-type seedlings were transferred to small pots, grown for 2 weeks under normal

conditions, and then subjected to drought treatment by withholding watering for 10 d.

For water loss treatment of detached leaves, shoots of 4-week-old mutant and wild-type plants were cut with a pair of scissors, placed on a piece of weighing paper, and kept at 20°C and 75% humidity in the light. The shoots were weighed immediately after they were cut and periodically thereafter. The percentage of water loss was calculated on the basis of the initial weight of the plants, with three replicate shoots for each assay.

For stomatal aperture assays, epidermal strips from rosette leaves of 4-week-old seedlings were examined with a light microscope (B5-223 IEP; Motic China Group). Stomatal apertures were measured with Motic software for three replicates, with three epidermal strips per replicate and 30 stomata per strip.

For Pro and sugar analysis, the shoots of 4-week-old seedlings were detached and kept on the greenhouse bench for 3 h. They were then ground in liquid nitrogen before Pro and carbohydrate contents were determined according to Chen et al. (2005).

Genetic Mapping and Mutant Complementation

abo6 (ecotype Columbia *gl1*) was crossed to *Ler* accession, and 1500 mutant plants were selected from the F2 population based on the ABA-sensitive phenotype on MS medium supplemented with 30 μM ABA. Simple sequence length polymorphism markers were used to map *ABO6* first to chromosome 5 between the BAC clones F8L15 and T20L5. Markers in MED24, T1E3, MUK11, MUG13, and K18I23 were then used to narrow the location of the *abo6* mutation to a region between the BAC clone MUK11 and MUG13. All candidate genes in this region were sequenced and a G–A point mutation was found in *AT5G04895*.

For complementation of the *abo6* mutant, *ABO6* cDNA was amplified from reverse-transcribed cDNA with the primer pair 5'-CTGCAGATGCGTTTCACAAAAGAATAAGCCTCTTC-3' and 5'-GGTACCTTACTTGCCCTTGGATCGCCTGC-3'. The PCR products were then cloned in the T-easy vector (Promega). The DNA fragments were then cloned in the *Pst*I and *Kpn*I sites of a modified vector pCAMBIA1300 under the control of a super promoter. The cloned construct was transformed into *Agrobacterium tumefaciens* GV3101 cells and transferred into plants using the floral dip method (Clough and Bent, 1998). Transgenic homozygous lines in the T3 generation were used for complementation.

A Salk T-DNA insertion line SALK_019865, obtained from the Arabidopsis Information Resource, was lethal in the homozygous state. *abo6* was crossed with the heterozygous T-DNA lines to obtain the F1 seedlings, and their sensitivity to ABA was examined. The genomic DNA fragments isolated from ABA-sensitive lines were examined by PCR analysis, and all lines were determined to be heterozygous mutants that contained both *abo6* and the SALK_019865 T-DNA insertion. The primers used for amplification of T-DNA insertion were as follows: LP, 5'-ATTGGTTCTCATGAGTGAC-3'; RP, 5'-GGTGGTCTCTTTGCTTTCC-3'; TF, 5'-ATTTTGCCGATTTCCGGAAC-3'. The primers used for amplification of *abo6* mutation were as follows: *abo6*-dcaps-F, 5'-TAGAGCGGGATATCTTCGCAATGC-3'; *abo6*-dcaps-R, 5'-TAACCGTTT-CACCAAGAGGAGCT-3'. The PCR products amplified from the wild type were cut with *Sac*I, whereas those amplified from *abo6* were not.

abo6 was also crossed with *abi1-1* and *abi2-1* and the double mutants were identified (Allen et al., 1999).

Subcellular Localization of ABO6

Full-length *ABO6* cDNA was obtained by PCR from the T-easy vector containing *ABO6* cDNA with the primers 5'-CTGCAGATGCGTTTCACAAAAGAATAAGCCTCTTC-3' and 5'-GGTACCTTGGCCTTGGATCGCCTGC-3'. The PCR products were then cloned into the pMD18 T-vector (TaKaRa); the DNA fragments were then subcloned into the *Pst*I and *Kpn*I

sites of a modified vector pCAMBIA1300 that contains GFP cDNA between the *KpnI* and *SacI* sites. The cloned construct was transformed into *Agrobacterium* GV3101 cells and transferred into plants using the floral dip method (Clough and Bent, 1998). Because GFP fluorescence was not observed in the transgenic plants, the N-terminal part of *ABO6* that contains the mitochondrial signal peptide was used in place of full-length *ABO6* cDNA using the primers 5'-CTGCAGATGCGTTTCACAAAAA-GAATAAGCCTCTTC-3' and 5'-GGTACCATCTGGACGCCGTGGAAGA-AG-3' in pCAMBIA1300-GFP. After sequence analysis, correct vectors were transformed into isolated *Arabidopsis* protoplasts, which were stained with the Mito-tracker and examined with a Zeiss LSM 510 META confocal microscope. For confocal microscopy, green (GFP) images were obtained with an excitation at 488 nm and emission at 525 nm, and red images (MitoTracker stain) were obtained with an excitation at 543 nm and emission at 615 nm.

ROS Assays

H₂O₂ was detected in situ by DAB staining (Thordal-Christensen et al., 1997). The terminal leaflet of the first fully expanded leaf was sampled from 28-d-old wild-type and *abo6* plants treated with 50 μM ABA or drought for 3 h. Leaflets were collected and vacuum-infiltrated with DAB solution (1 mg/mL, pH 3.8; Sigma-Aldrich). The sampled leaflets were placed in a plastic box in a light homoeothermic incubator until a reddish-brown precipitate was observed (8 h); they were then fixed in a solution of 3:1:1 ethanol:lactic acid:glycerol and photographed. In the roots, H₂O₂ was stained with 0.1 mg/mL DAB in 50 mM Tris buffer, pH 5.0 (Benitez-Alfonso et al., 2009), with subsequent steps being the same as those described for leaflets.

The DCFH-DA staining assay was performed as described previously (Liu et al., 2010). Briefly, 4-d-old seedlings were treated with 0 or 50 μM ABA for 5 h, incubated in 50 μM DCFH-DA in 20 mM K-phosphate, pH 6.0, in darkness for 10 min, and washed three times with the same buffer. Fluorescence was detected with a confocal microscope (Zeiss LSM 510 META) with an excitation at 488 nm and emission at 525 nm and collected by scanning different slices from the bottom to the top of a sample. The slices were overlaid using the projection function of Zeiss LSM Image Browser software, and the fluorescence intensities were collected using AxioVision Rel. 4.8 software, which was displayed as estimated mean pixel intensities. Approximately 20 images were acquired per sample, and three independent experiments were performed.

We used NBT staining to detect O₂⁻ in situ as described previously (Dunand et al., 2007), with the following modifications. Four-day-old seedlings were treated with 0 or 50 μM ABA for 5 h, incubated in 2 mM NBT in 20 mM K-phosphate with 0.1 M NaCl at pH 6.1 for 15 min, and then transferred to distilled water. Root tips were imaged under bright-field illumination on a Zeiss Scope AI microscope, and all of the images in an experiment were taken with the same settings. Approximately 20 images were taken each time, and three independent experiments were performed.

Determination of GSH Content

Four-day-old seedlings were transferred to MS medium containing 30 μM ABA and 1 mM BSO and grown for another 7 d. Then, root tips were collected for quantitative measurement of GSH. The GSH content was measured using a Glutathione Colorimetric Detection Kit (BioVision), with the following minor modifications (Su et al., 2011). The root tips were ground to powder using liquid nitrogen, ~50 mg of each sample was then dissolved in 400 μL GSH buffer, and 100 μL 5% sulfosalicylic acid was added and mixed gently. The samples were incubated on ice for 5 min and centrifuged at 12,000g at 4°C for 15 min, and the supernatants were collected for GSH detection.

For determination of GSH content, the samples or GSH standards (20 μL) were mixed with 160 μL of reaction solution (20 μL NADPH generating mix

and 140 μL glutathione reaction buffer) on a microtiter plate and incubated at room temperature for 10 min. Then, 20 μL of substrate was added to each sample, and the absorbencies at 405 nm were recorded for 5, 10, 20, and 30 min. The GSH content was calculated according to the standard curve.

RNA Gel Blot Analysis and Quantitative RT-PCR

Two-week-old seedlings were submerged into 50 μM ABA for 5 h. Total RNAs were extracted and hybridized with different probes as described previously (Liu et al., 2010). The primers used to amplify the probes for RNA gel blot analysis are listed in Supplemental Table 1 online.

For real-time qRT-PCR, ~4 μg of total RNAs was digested with RNase-free DNase I. The digested RNA was then reverse transcribed into cDNA using oligo(dT) primers (Promega) and Moloney Murine Leukemia Virus Transcriptase (Promega) in a 20-μL reaction. The cDNAs were used as templates in real-time PCR reactions using SYBR Premix Ex Tag (TaKaRa) with gene-specific primers and the internal control (*ACTIN2/8*). The primers used for qRT-PCR are listed in Supplemental Table 2 online; the primers were used to amplify *NAD1b*, *NAD1c*, *NAD2b*, *NAD4*, and *NAD5a* are listed in Supplemental Table 1 online (Liu et al., 2010). PCR was performed using a PTC-200 DNA engine cycle (MJ Research) with a Chrom4 detector in 20-μL reactions and the following amplification procedure: 5 min at 95°C (one cycle), 15 s at 95°C, 15 s at 57 to 60°C, 20 s at 72°C (40 cycles), and 5 min at 72°C. Next, a standard dissociation protocol was used to examine whether the amplifications were specific. Triple biological replications were performed for each of three independent samples, and the values shown represent the average of three assays for each real-time PCR sample. The results are given as a ratio of the values in the wild type.

For the analysis of NAD splicing, the primers were designed to amplify two different fragments (de Longevialle et al., 2007). One pair of primers was used to amplify the fragment that spans two adjacent exons (to quantify spliced mRNA); another pair of primers was used to amplify the intron-exon fragment (to quantify unspliced mRNA). These primers are listed in Supplemental Table 3 online. If amplification of the intron-exon fragment in *abo6* was greater than that in the wild type, it means that the splicing was impaired in *abo6*.

Marker Gene Analysis

Arabidopsis plants harboring *ProDR5:GUS*, *ProIAA2:GUS*, *ProAUX1:AUX1-YFP*, *ProPIN1:PIN1-GFP*, *ProPIN2:PIN2-GFP* (Wang et al., 2011), and *Mito-cpYFP* were crossed with *abo6*. Homozygous plants for the mutant and marker lines were separated from the F₂ and F₃ population before they were subjected to GUS staining or GFP. Four-day-old seedlings were transferred to MS containing 30 μM ABA, 600 μM GSH, or 2.5 mM BSO and grown for another 2 d.

For GUS staining, seedlings were incubated in 0.1 M phosphate buffer (a mixture of KH₂PO₄ and K₂HPO₄, pH 7.0) and 5 mg/mL X-Gluc at 37°C for different times and were then incubated in 75% ethanol for several hours to remove chlorophylls. Staining time was 40 min for *ProIAA2:GUS* and 24 h for *ProDR5:GUS*. Seedlings were photographed with an Olympus stereofluorescence microscope (SZX16 -DP72) and a Zeiss Scope AI microscope.

For GFP fluorescence, the roots of the plants treated with different reagents were observed with a Zeiss LSM 510 META confocal microscope and photographed under the same settings. The fluorescence images were collected by scanning different slices from one side to the other side, and the images were overlaid using the projection function of Zeiss LSM image browser software. Fluorescence intensities were collected using AxioVision Rel. 4.8 software, which was displayed as estimated mean pixel intensities. Approximately 20 images were taken per sample, and three independent experiments were performed.

Accession Numbers

Sequence data from this article can be found in the Arabidopsis Genome Initiative or GenBank/EMBL databases under the following accession numbers: ABO6, At5g04895; ABO5, At1g51965; NDUFS4, At1g47260; ATRBOHF, At1g64060; ABI1, At4g26080; ABI2, At5g57050; AOX1a, At3g22370; NDB2, At4g05020; NDB3, At4g21490; NDB4, At2g20800; RD29A, At5g52310; ACTIN2, At3g18780; ACTIN8, At1g49240; TUB4, At5g44340; RPL2, Atmg00560; COX2, Atmg00160; CCB452, Atmg00180; RPS3, Atmg00090; NAD1B, Atmg01120; NAD1C, Atmg00516; NAD2A, Atmg00285; NAD2B, Atmg01320; NAD4, Atmg00580; NAD5A, Atmg00513; NAD5C, Atmg00060; and NAD7, Atmg00510.

Supplemental Data

The following materials are available in the online version of this article.

Supplemental Figure 1. The Growth Phenotype of *abo6*.

Supplemental Figure 2. Seed Germination and Root Growth of *ndufs4* and *abo5* on ABA Containing MS Medium Supplemented with GSH or DTT.

Supplemental Figure 3. Seed Germination and Root Growth of *abo6*, the Wild Type, *Ler*, *abi1-1*, *abi2-1*, *abo6 abi1-1*, and *abo6 abi2-1* in Response to ABA.

Supplemental Figure 4. GSH Contents in the Roots of Different Phenotypes under ABA and No ABA Treatments.

Supplemental Table 1. Primers Used to Amplify Fragments in RNA Gel Blots.

Supplemental Table 2. Primers Used for qRT-PCR.

Supplemental Table 3. Primers Used for the Splicing qRT-PCR Experiment of Mitochondrial Transcripts.

ACKNOWLEDGMENTS

This work was supported by grants from the National Nature Science Foundation of China (91117017 and 31121002), the National Basic Research Program of China (973 Program; 2012CB114300), the National Transgenic Research Project (2011ZX08009-002), and the China Postdoctoral Science Foundation-funded project (2011M500453). We thank Miguel Angel Torres (University of North Carolina at Chapel Hill) for providing *atrbohF* mutant seeds, Chuanyou Li (Institute of Genetics and Developmental Biology) for providing various auxin related materials, and the ABRC for providing the T-DNA insertion lines of ABO6.

AUTHOR CONTRIBUTIONS

J.H. and Z.G. designed the experiment. J.H. performed the majority of experiments and analyzed the data. Y.D., D.H., G.F., L.W., Y.L., Z.C., and L.-J.Q. assisted with the experiment and data analyses. L.H. assisted with the experiments. J.H. and Z.G. wrote the article.

Received March 28, 2012; revised March 28, 2012; accepted May 9, 2012; published May 31, 2012.

REFERENCES

Allen, G.J., Kuchitsu, K., Chu, S.P., Murata, Y., and Schroeder, J.I. (1999). *Arabidopsis* *abi1-1* and *abi2-1* phosphatase mutations

reduce abscisic acid-induced cytoplasmic calcium rises in guard cells. *Plant Cell* **11**: 1785–1798.

Apel, K., and Hirt, H. (2004). Reactive oxygen species: metabolism, oxidative stress, and signal transduction. *Annu. Rev. Plant Biol.* **55**: 373–399.

Bai, L., Zhang, G., Zhou, Y., Zhang, Z., Wang, W., Du, Y., Wu, Z., and Song, C.P. (2009). Plasma membrane-associated proline-rich extensin-like receptor kinase 4, a novel regulator of Ca signalling, is required for abscisic acid responses in *Arabidopsis thaliana*. *Plant J.* **60**: 314–327.

Bashandy, T., Guilleminot, J., Vernoux, T., Caparros-Ruiz, D., Ljung, K., Meyer, Y., and Reichheld, J.P. (2010). Interplay between the NADP-linked thioredoxin and glutathione systems in *Arabidopsis* auxin signaling. *Plant Cell* **22**: 376–391.

Belin, C., Megies, C., Hauserová, E., and Lopez-Molina, L. (2009). Abscisic acid represses growth of the *Arabidopsis* embryonic axis after germination by enhancing auxin signaling. *Plant Cell* **21**: 2253–2268.

Benitez-Alfonso, Y., Cilia, M., San Roman, A., Thomas, C., Maule, A., Hearn, S., and Jackson, D. (2009). Control of *Arabidopsis* meristem development by thioredoxin-dependent regulation of intercellular transport. *Proc. Natl. Acad. Sci. USA* **106**: 3615–3620.

Benjamins, R., and Scheres, B. (2008). Auxin: The looping star in plant development. *Annu. Rev. Plant Biol.* **59**: 443–465.

Benková, E., Michniewicz, M., Sauer, M., Teichmann, T., Seifertová, D., Jürgens, G., and Friml, J. (2003). Local, efflux-dependent auxin gradients as a common module for plant organ formation. *Cell* **115**: 591–602.

Boudet, N., Aubourg, S., Toffano-Nioche, C., Kreis, M., and Lecharny, A. (2001). Evolution of intron/exon structure of DEAD helicase family genes in *Arabidopsis*, *Caenorhabditis*, and *Drosophila*. *Genome Res.* **11**: 2101–2114.

Brady, S.M., Sarkar, S.F., Bonetta, D., and McCourt, P. (2003). The ABCISIC ACID INSENSITIVE 3 (ABI3) gene is modulated by far-nylation and is involved in auxin signaling and lateral root development in *Arabidopsis*. *Plant J.* **34**: 67–75.

Chen, Z., Hong, X., Zhang, H., Wang, Y., Li, X., Zhu, J.K., and Gong, Z. (2005). Disruption of the cellulose synthase gene, *AtCesA8/IRX1*, enhances drought and osmotic stress tolerance in *Arabidopsis*. *Plant J.* **43**: 273–283.

Chinnusamy, V., Gong, Z., and Zhu, J.K. (2008). Abscisic acid-mediated epigenetic processes in plant development and stress responses. *J. Integr. Plant Biol.* **50**: 1187–1195.

Clifton, R., Lister, R., Parker, K.L., Sappl, P.G., Elhafez, D., Millar, A.H., Day, D.A., and Whelan, J. (2005). Stress-induced co-expression of alternative respiratory chain components in *Arabidopsis thaliana*. *Plant Mol. Biol.* **58**: 193–212.

Clough, S.J., and Bent, A.F. (1998). Floral dip: a simplified method for *Agrobacterium*-mediated transformation of *Arabidopsis thaliana*. *Plant J.* **16**: 735–743.

Cutler, S.R., Rodriguez, P.L., Finkelstein, R.R., and Abrams, S.R. (2010). Abscisic acid: Emergence of a core signaling network. *Annu. Rev. Plant Biol.* **61**: 651–679.

de Longevialle, A.F., Meyer, E.H., Andrés, C., Taylor, N.L., Lurin, C., Millar, A.H., and Small, I.D. (2007). The pentatricopeptide repeat gene *OTP43* is required for trans-splicing of the mitochondrial *nad1* Intron 1 in *Arabidopsis thaliana*. *Plant Cell* **19**: 3256–3265.

Dunand, C., Crèvecoeur, M., and Penel, C. (2007). Distribution of superoxide and hydrogen peroxide in *Arabidopsis* root and their influence on root development: Possible interaction with peroxidases. *New Phytol.* **174**: 332–341.

Foreman, J., Demidchik, V., Bothwell, J.H., Mylona, P., Miedema, H., Torres, M.A., Linstead, P., Costa, S., Brownlee, C., Jones,

- J.D., Davies, J.M., and Dolan, L.** (2003). Reactive oxygen species produced by NADPH oxidase regulate plant cell growth. *Nature* **422**: 442–446.
- Fukaki, H., and Tasaka, M.** (2009). Hormone interactions during lateral root formation. *Plant Mol. Biol.* **69**: 437–449.
- Garmier, M., Carroll, A.J., Delannoy, E., Vallet, C., Day, D.A., Small, I.D., and Millar, A.H.** (2008). Complex I dysfunction redirects cellular and mitochondrial metabolism in *Arabidopsis*. *Plant Physiol.* **148**: 1324–1341.
- Gazarian, I.G., Lagrimini, L.M., Mellon, F.A., Naldrett, M.J., Ashby, G.A., and Thorneley, R.N.** (1998). Identification of skatolyl hydroperoxide and its role in the peroxidase-catalysed oxidation of indol-3-yl acetic acid. *Biochem. J.* **333**: 223–232.
- Gong, Z., Dong, C.H., Lee, H., Zhu, J., Xiong, L., Gong, D., Stevenson, B., and Zhu, J.K.** (2005). A DEAD box RNA helicase is essential for mRNA export and important for development and stress responses in *Arabidopsis*. *Plant Cell* **17**: 256–267.
- Gong, Z., Lee, H., Xiong, L., Jagendorf, A., Stevenson, B., and Zhu, J.K.** (2002). RNA helicase-like protein as an early regulator of transcription factors for plant chilling and freezing tolerance. *Proc. Natl. Acad. Sci. USA* **99**: 11507–11512.
- Gutierrez, S., Sabar, M., Lelandais, C., Chetrit, P., Diolez, P., Degand, H., Boutry, M., Vedel, F., de Kouchkovsky, Y., and De Paepe, R.** (1997). Lack of mitochondrial and nuclear-encoded subunits of complex I and alteration of the respiratory chain in *Nicotiana glauca* mitochondrial deletion mutants. *Proc. Natl. Acad. Sci. USA* **94**: 3436–3441.
- Kant, P., Kant, S., Gordon, M., Shaked, R., and Barak, S.** (2007). STRESS RESPONSE SUPPRESSOR1 and STRESS RESPONSE SUPPRESSOR2, two DEAD-box RNA helicases that attenuate *Arabidopsis* responses to multiple abiotic stresses. *Plant Physiol.* **145**: 814–830.
- Kim, T.H., Böhmer, M., Hu, H., Nishimura, N., and Schroeder, J.I.** (2010). Guard cell signal transduction network: Advances in understanding abscisic acid, CO₂, and Ca²⁺ signaling. *Annu. Rev. Plant Biol.* **61**: 561–591.
- Köhler, D., Schmidt-Gattung, S., and Binder, S.** (2010). The DEAD-box protein PMH2 is required for efficient group II intron splicing in mitochondria of *Arabidopsis thaliana*. *Plant Mol. Biol.* **72**: 459–467.
- Koprivova, A., des Fracs-Small, C.C., Calder, G., Mugford, S.T., Tanz, S., Lee, B.R., Zechmann, B., Small, I., and Kopriva, S.** (2010b). Identification of a pentatricopeptide repeat protein implicated in splicing of intron 1 of mitochondrial nad7 transcripts. *J. Biol. Chem.* **285**: 32192–32199.
- Koprivova, A., Mugford, S.T., and Kopriva, S.** (2010a). *Arabidopsis* root growth dependence on glutathione is linked to auxin transport. *Plant Cell Rep.* **29**: 1157–1167.
- Kwak, J.M., Mori, I.C., Pei, Z.M., Leonhardt, N., Torres, M.A., Dangi, J.L., Bloom, R.E., Bodde, S., Jones, J.D., and Schroeder, J.I.** (2003). NADPH oxidase *AtrbohD* and *AtrbohF* genes function in ROS-dependent ABA signaling in *Arabidopsis*. *EMBO J.* **22**: 2623–2633.
- Laloi, C., Apel, K., and Danon, A.** (2004). Reactive oxygen signalling: The latest news. *Curr. Opin. Plant Biol.* **7**: 323–328.
- Lee, B.H., Lee, H., Xiong, L., and Zhu, J.K.** (2002). A mitochondrial complex I defect impairs cold-regulated nuclear gene expression. *Plant Cell* **14**: 1235–1251.
- Leung, J., Bouvier-Durand, M., Morris, P.C., Guerrier, D., Chedford, F., and Giraudat, J.** (1994). *Arabidopsis* ABA response gene *ABI1*: features of a calcium-modulated protein phosphatase. *Science* **264**: 1448–1452.
- Leung, J., Merlot, S., and Giraudat, J.** (1997). The *Arabidopsis* *ABSCISIC ACID-INSENSITIVE2 (ABI2)* and *ABI1* genes encode homologous protein phosphatases 2C involved in abscisic acid signal transduction. *Plant Cell* **9**: 759–771.
- Liu, P.P., Montgomery, T.A., Fahlgren, N., Kasschau, K.D., Nonogaki, H., and Carrington, J.C.** (2007). Repression of AUXIN RESPONSE FACTOR10 by microRNA160 is critical for seed germination and post-germination stages. *Plant J.* **52**: 133–146.
- Liu, Y., He, J., Chen, Z., Ren, X., Hong, X., and Gong, Z.** (2010). *ABA overly-sensitive 5 (ABO5)*, encoding a pentatricopeptide repeat protein required for cis-splicing of mitochondrial nad2 intron 3, is involved in the abscisic acid response in *Arabidopsis*. *Plant J.* **63**: 749–765.
- Maxwell, D.P., Wang, Y., and McIntosh, L.** (1999). The alternative oxidase lowers mitochondrial reactive oxygen production in plant cells. *Proc. Natl. Acad. Sci. USA* **96**: 8271–8276.
- Meinhard, M., and Grill, E.** (2001). Hydrogen peroxide is a regulator of ABI1, a protein phosphatase 2C from *Arabidopsis*. *FEBS Lett.* **508**: 443–446.
- Meinhard, M., Rodriguez, P.L., and Grill, E.** (2002). The sensitivity of ABI2 to hydrogen peroxide links the abscisic acid-response regulator to redox signalling. *Planta* **214**: 775–782.
- Meyer, K., Leube, M.P., and Grill, E.** (1994). A protein phosphatase 2C involved in ABA signal transduction in *Arabidopsis thaliana*. *Science* **264**: 1452–1455.
- Miao, Y., Lv, D., Wang, P., Wang, X.C., Chen, J., Miao, C., and Song, C.P.** (2006). An *Arabidopsis* glutathione peroxidase functions as both a redox transducer and a scavenger in abscisic acid and drought stress responses. *Plant Cell* **18**: 2749–2766.
- Mingam, A., Toffano-Nioche, C., Brunaud, V., Boudet, N., Kreis, M., and Lecharny, A.** (2004). DEAD-box RNA helicases in *Arabidopsis thaliana*: Establishing a link between quantitative expression, gene structure and evolution of a family of genes. *Plant Biotechnol. J.* **2**: 401–415.
- Monroe-Augustus, M., Zolman, B.K., and Bartel, B.** (2003). IBR5, a dual-specificity phosphatase-like protein modulating auxin and abscisic acid responsiveness in *Arabidopsis*. *Plant Cell* **15**: 2979–2991.
- Murata, Y., Pei, Z.M., Mori, I.C., and Schroeder, J.** (2001). Abscisic acid activation of plasma membrane Ca(2+) channels in guard cells requires cytosolic NAD(P)H and is differentially disrupted upstream and downstream of reactive oxygen species production in *abi1-1* and *abi2-1* protein phosphatase 2C mutants. *Plant Cell* **13**: 2513–2523.
- Nakagami, H., Soukupová, H., Schikora, A., Zárský, V., and Hirt, H.** (2006). A mitogen-activated protein kinase kinase mediates reactive oxygen species homeostasis in *Arabidopsis*. *J. Biol. Chem.* **281**: 38697–38704.
- Nakashima, K., Fujita, Y., Kanamori, N., Katagiri, T., Umezawa, T., Kidokoro, S., Maruyama, K., Yoshida, T., Ishiyama, K., Kobayashi, M., Shinozaki, K., and Yamaguchi-Shinozaki, K.** (2009). Three *Arabidopsis* SnRK2 protein kinases, SRK2D/SnRK2.2, SRK2E/SnRK2.6/OST1 and SRK2I/SnRK2.3, involved in ABA signaling are essential for the control of seed development and dormancy. *Plant Cell Physiol.* **50**: 1345–1363.
- Potters, G., Pasternak, T.P., Guisez, Y., Palme, K.J., and Jansen, M.A.** (2007). Stress-induced morphogenic responses: growing out of trouble? *Trends Plant Sci.* **12**: 98–105.
- Ren, X., Chen, Z., Liu, Y., Zhang, H., Zhang, M., Liu, Q., Hong, X., Zhu, J.K., and Gong, Z.** (2010). ABO3, a WRKY transcription factor, mediates plant responses to abscisic acid and drought tolerance in *Arabidopsis*. *Plant J.* **63**: 417–429.
- Shibasaki, K., Uemura, M., Tsurumi, S., and Rahman, A.** (2009). Auxin response in *Arabidopsis* under cold stress: Underlying molecular mechanisms. *Plant Cell* **21**: 3823–3838.

- Sirichandra, C., Gu, D., Hu, H.C., Davanture, M., Lee, S., Djaoui, M., Valot, B., Zivy, M., Leung, J., Merlot, S., and Kwak, J.M. (2009). Phosphorylation of the *Arabidopsis* AtrbohF NADPH oxidase by OST1 protein kinase. *FEBS Lett.* **583**: 2982–2986.
- Stonebloom, S., Burch-Smith, T., Kim, I., Meinke, D., Mindrinos, M., and Zambryski, P. (2009). Loss of the plant DEAD-box protein ISE1 leads to defective mitochondria and increased cell-to-cell transport via plasmodesmata. *Proc. Natl. Acad. Sci. USA* **106**: 17229–17234.
- Su, T., Xu, J., Li, Y., Lei, L., Zhao, L., Yang, H., Feng, J., Liu, G., and Ren, D. (2011). Glutathione-indole-3-acetonitrile is required for camalexin biosynthesis in *Arabidopsis thaliana*. *Plant Cell* **23**: 364–380.
- Sung, T.Y., Tseng, R.C.C., and Hsieh, M.H. (2010). The SLO1 PPR protein is required for RNA editing at multiple sites with similar upstream sequences in *Arabidopsis* mitochondria. *Plant J.* **63**: 499–511.
- Teale, W.D., Ditengou, F.A., Dovzhenko, A.D., Li, X., Molendijk, A.M., Ruperti, B., Paponov, I., and Palme, K. (2008). Auxin as a model for the integration of hormonal signal processing and transduction. *Mol. Plant* **1**: 229–237.
- Thordal-Christensen, H., Zhang, Z., Wei, Y., and Collinge, D.B. (1997). Subcellular localization of H₂O₂ in plants. H₂O₂ accumulation in papillae and hypersensitive response during the barley-powdery mildew interaction. *Plant J.* **11**: 1187–1194.
- Tiryaki, I., and Staswick, P.E. (2002). An *Arabidopsis* mutant defective in jasmonate response is allelic to the auxin-signaling mutant *axr1*. *Plant Physiol.* **130**: 887–894.
- Tognetti, V.B. et al. (2010). Perturbation of indole-3-butyric acid homeostasis by the UDP-glucosyltransferase UGT74E2 modulates *Arabidopsis* architecture and water stress tolerance. *Plant Cell* **22**: 2660–2679.
- Ton, J., Flors, V., and Mauch-Mani, B. (2009). The multifaceted role of ABA in disease resistance. *Trends Plant Sci.* **14**: 310–317.
- Tsakagoshi, H., Busch, W., and Benfey, P.N. (2010). Transcriptional regulation of ROS controls transition from proliferation to differentiation in the root. *Cell* **143**: 606–616.
- Ulmason, T., Murfett, J., Hagen, G., and Guilfoyle, T.J. (1997). Aux/IAA proteins repress expression of reporter genes containing natural and highly active synthetic auxin response elements. *Plant Cell* **9**: 1963–1971.
- Unsold, M., Marienfeld, J.R., Brandt, P., and Brennicke, A. (1997). The mitochondrial genome of *Arabidopsis thaliana* contains 57 genes in 366,924 nucleotides. *Nat. Genet.* **15**: 57–61.
- Vernoux, T., Wilson, R.C., Seeley, K.A., Reichheld, J.P., Muroy, S., Brown, S., Maughan, S.C., Cobbett, C.S., Van Montagu, M., Inzé, D., May, M.J., and Sung, Z.R. (2000). The *ROOT MERISTEMLESS1/CADMIUM SENSITIVE2* gene defines a glutathione-dependent pathway involved in initiation and maintenance of cell division during post-embryonic root development. *Plant Cell* **12**: 97–110.
- Wang, L., Hua, D., He, J., Duan, Y., Chen, Z., Hong, X., and Gong, Z. (2011). Auxin Response Factor2 (ARF2) and its regulated homeo-domain gene *HB33* mediate abscisic acid response in *Arabidopsis*. *PLoS Genet.* **7**: e1002172.
- Wang, W. et al. (2008). Superoxide flashes in single mitochondria. *Cell* **134**: 279–290.
- Wilson, A.K., Pickett, F.B., Turner, J.C., and Estelle, M. (1990). A dominant mutation in *Arabidopsis* confers resistance to auxin, ethylene and abscisic acid. *Mol. Gen. Genet.* **222**: 377–383.
- Xiong, L., and Zhu, J.K. (2003). Regulation of abscisic acid biosynthesis. *Plant Physiol.* **133**: 29–36.
- Yin, H., Zhang, X., Liu, J., Wang, Y., He, J., Yang, T., Hong, X., Yang, Q., and Gong, Z. (2009). Epigenetic regulation, somatic homologous recombination, and abscisic acid signaling are influenced by DNA polymerase epsilon mutation in *Arabidopsis*. *Plant Cell* **21**: 386–402.
- Zhang, W., Qin, C., Zhao, J., and Wang, X. (2004). Phospholipase D alpha 1-derived phosphatidic acid interacts with ABI1 phosphatase 2C and regulates abscisic acid signaling. *Proc. Natl. Acad. Sci. USA* **101**: 9508–9513.
- Zhang, Y., Zhu, H., Zhang, Q., Li, M., Yan, M., Wang, R., Wang, L., Welti, R., Zhang, W., and Wang, X. (2009). Phospholipase alpha1 and phosphatidic acid regulate NADPH oxidase activity and production of reactive oxygen species in ABA-mediated stomatal closure in *Arabidopsis*. *Plant Cell* **21**: 2357–2377.
- Zhou, X., Hua, D., Chen, Z., Zhou, Z., and Gong, Z. (2009). Elongator mediates ABA responses, oxidative stress resistance and anthocyanin biosynthesis in *Arabidopsis*. *Plant J.* **60**: 79–90.
- Zhu, J.K. (2002). Salt and drought stress signal transduction in plants. *Annu. Rev. Plant Biol.* **53**: 247–273.